Journal of Palaeogeography

ORIGINAL ARTICLE Open Access

First steps in reconstructing Early Jurassic sea water temperatures in the Andean Basin of northern Chile based on stable isotope analyses of oyster and brachiopod shells

Matthias Alberti[1*], Franz T. Fürsich[2] and Nils Andersen[3]

Abstract

The stable isotope ($\delta^{13}C$, $\delta^{18}O$) composition of a collection of Lower Jurassic brachiopods and oysters from the Andean Basin of northern Chile was analyzed. The results allow the first reconstruction of absolute water temperatures for several ammonite zones in the Lower Jurassic of South America. The temperature record starts with comparatively high values in the Late Sinemurian (average: 27.0 °C; Raricostatum Zone). Just before the Sinemurian–Pliensbachian transition, temperatures dropped to an average of 24.3 °C. The lowest temperature value in the dataset was recorded for a brachiopod shell of the latest Pliensbachian Spinatum Zone (19.6 °C). No data are available for the Early Toarcian, but results for the late Toarcian show again comparatively warm conditions (average: 24.4 °C; Thouarsense–Levesquei zones). Even though more material and analyses are necessary to corroborate the recorded temperatures, the present dataset seems to indicate the global nature of the Late Pliensbachian Cooling Event. In contrast, the global warming during the Toarcian Oceanic Anoxic Event has not been recorded due to a lack of Early Toarcian material. The $\delta^{13}C$ record of brachiopods and oysters documents a gradual increase in values representing background conditions. Oyster shells were used for high-resolution stable isotope analyses and show seasonal temperature fluctuations over a period of around 3 years in the life time of the bivalves. If explained only by temperatures, the $\delta^{18}O$ values point to a minimum estimate for the seasonality in the late Toarcian of slightly more than 3 °C.

Keywords: Early Jurassic, Chile, Stable isotopes, Palaeoclimate, Water temperatures, Seasonality

1 Introduction

The climate conditions of the Jurassic world have traditionally been described as warmer than today, relatively stable through time, and with weak latitudinal temperature gradients leading to a lack of polar glaciations (e.g., Chandler et al. 1992; Valdes and Sellwood 1992; Rees et al. 2000; Hallam 2001; Bailey et al. 2003; Sellwood and Valdes 2006). In the last few decades, this simple view has been challenged by a series of articles, suggesting polar ice caps for at least short intervals in the Jurassic (e.g., Price 1999; Dromart et al. 2003; Suan et al. 2008, 2010) and larger temperature fluctuations (e.g., Dera et al. 2011; Korte et al. 2015; Martinez and Dera 2015; Silva and Duarte 2015; Price et al. 2016). Only recently, Alberti et al. (2017, 2019) presented data pointing to latitudinal temperature gradients in the Middle and Late Jurassic as steep as today. Much of our knowledge on the Jurassic climate is based on seawater temperature reconstructions using stable isotope ($\delta^{18}O$) analyses of fossil hard parts. This methodology has been fundamental in improving our understanding of the climate throughout the history of Earth (e.g., Epstein et al. 1951; Urey et al. 1951). During the last decades a

* Correspondence: matthias.alberti@ifg.uni-kiel.de
[1]Institut für Geowissenschaften, Christian-Albrechts-Universität zu Kiel, Ludewig-Meyn-Straße 10, 24118 Kiel, Germany
Full list of author information is available at the end of the article

large amount of data has been assembled by analyzing mainly calcitic fossils such as belemnite rostra and bivalve or brachiopod shells. However, research on temperature reconstructions has concentrated largely on European localities with data from other regions of the Earth being relatively scarce and scattered. Consequently, it seems beneficial to gather more information from non-European sections in order to fully understand global climate conditions in the Jurassic. The present study is part of a series of articles trying to improve our knowledge of the seawater temperature conditions of Gondwanan localities (Alberti et al. 2012a, 2012b, 2013, 2017, 2019).

The Early Jurassic was an epoch which experienced several events with a global impact. Most of these have been identified via geochemical analyses of sedimentary rocks or their fossil content (e.g., Jenkyns 1988; Hesselbo et al. 2000a; Jenkyns et al. 2002; Korte et al. 2009; Bodin et al. 2016) and could be connected to pulses in the volcanic activity of the Karoo-Ferrar large igneous province influencing the atmospheric composition and thus the global climate. The strongest of these events was the Toarcian Oceanic Anoxic Event (TOAE) which is evident in the geological record by a prominent carbon isotope excursion and has been studied thoroughly over the last decades (e.g., Jenkyns 1988; Mettraux et al. 1989; Hesselbo et al. 2000a, 2007; McArthur et al. 2000; Schmid-Röhl et al. 2002; van de Schootbrugge et al. 2005a; Metodiev and Koleva-Rekalova 2008; Suan et al. 2008; Rodríguez-Tovar and Reolid 2013; Huang and Hesselbo 2014; Ullmann et al. 2014; Ruhl et al. 2016; Bougeault et al. 2017). Following a phase of very low temperatures during the Late Pliensbachian, increased volcanic activity in the Early Toarcian in combination with other factors (such as the release of methane hydrates from continental shelfs; Hesselbo et al. 2000a) seems to have caused perturbations in the carbon cycle, intense global warming, ocean acidification, and ultimately mass extinctions (e.g., Aberhan and Fürsich 1996; Pálfy and Smith 2000; Aberhan and Baumiller 2003; Cecca and Macchioni 2004; Gómez et al. 2008; Dera et al. 2010; Dera and Donnadieu 2012; Danise et al. 2013; Huang and Hesselbo 2014; Krencker et al. 2014). While the global nature of many of the Early Jurassic events (particularly the TOAE) has been illustrated by geochemical analyses of rocks outside Europe (e.g., Al-Suwaidi et al. 2010, 2014, 2016; Mazzini et al. 2010; Caruthers et al. 2011; Gröcke et al. 2011; Suan et al. 2011; Yi et al. 2013; Kemp and Izumi 2014; Ros-Franch et al. 2019), reconstructions of absolute water temperatures for the Early Jurassic are almost completely restricted to the northwestern Tethys. In the present study, a collection of Sinemurian to Toarcian oyster and brachiopod shells from the Andean Basin of Chile has been analyzed for their stable isotope ($\delta^{13}C$, $\delta^{18}O$) content in a first step to remedy this lack of data.

2 Geological overview

During the Mesozoic, a narrow but long back-arc basin existed along the South American Pacific margin more or less parallel to the modern-day Andes (e.g., Gröschke et al. 1988). This Andean Basin in present-day Chile and Argentina was divided into subbasins by several ridges and separated from the open ocean by volcanic arcs, but connections allowing the exchange of water masses existed most of the time (e.g., Gröschke et al. 1988; Aberhan 1992; Vicente 2006). A marine transgression reached the basin in the Late Triassic and marine conditions prevailed throughout the Jurassic (Aberhan 1992) with sea-level maxima in the Toarcian and Bajocian (Fantasia et al. 2018). The study area was inundated in the Early Sinemurian (von Hillebrandt 1971, 1973). The thickness of the Lower and Middle Jurassic successions (up to the basal Callovian) is more than 1000 m in the west, but only 30–40 m in the east (Aberhan 1992; von Hillebrandt 2002). The sampled Lower Jurassic strata belong to the Montandón Formation (Pérez 1982).

The fossil material used in the current study comes from four sections measured in detail by Aberhan (1992; sections with sample positions are illustrated in chapter 5). Section 2 was measured near Potrerillos (Fig. 1c), while sections 4, 5, and 6 were measured around El Transito approximately 280 km further south (Fig. 1d; compare Aberhan 1992). Their exact palaeogeographic position differs between the different available reconstructions, but was probably somewhere in the subtropical zone between 20°S to 35°S during the studied time interval (based on the Paleolatitude Calculator; van Hinsbergen et al. 2015). The analyzed specimens come from 22 horizons within the four sections and have a Sinemurian to Toarcian age.

As in other regions, the Jurassic biostratigraphy of South America relies heavily on ammonites, but age assignments and correlations based on these index fossils are still continuously improved and have not been finalized for all localities and/or time intervals (compare von Hillebrandt 1987; Riccardi 2008). The fossils used in the current study have been assigned to ammonite zones based on results of previous studies (von Hillebrandt 1973, 1987, 2002; von Hillebrandt and Schmidt-Effing 1981; Aberhan and von Hillebrandt 1996; Pérez et al. 2008; Fantasia et al. 2018).

Sinemurian ammonites of Chile were discussed in detail by von Hillebrandt (2002). The lower part of the Jurassic succession near El Transito contains only few ammonites, but von Hillebrandt (2002) described some specimens, which he could assign to the Raricostatum Zone. Even though the Sinemurian at these localities has

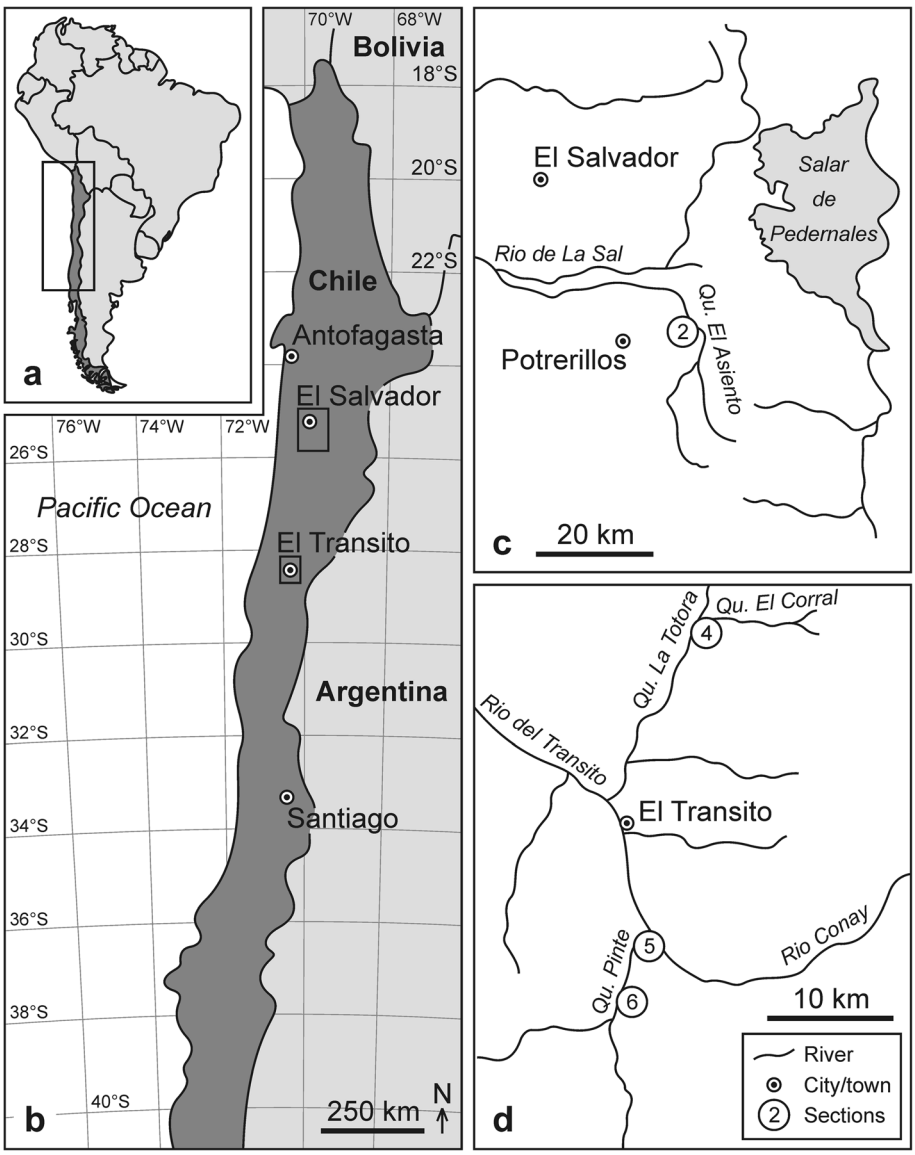

Fig. 1 a-d Schematic maps illustrating the position of the studied sections in northern Chile (modified after Aberhan 1992)

a thickness of more than 200 m, it seems to belong entirely to this ammonite zone indicating a late Sinemurian age (von Hillebrandt 2002).

Section 2 is a classic locality in the lower Quebrada El Asiento near Potrerillos examined or mentioned by numerous previous researchers (e.g., von Hillebrandt and Schmidt-Effing 1981; Pérez 1982; Aberhan 1992; von Hillebrandt 2006; Pérez et al. 2008; Fantasia et al. 2018). Shells used in the present study were collected from the Pliensbachian part of the succession, which was divided into three ammonite zones by von Hillebrandt and Schmidt-Effing (1981): Fig. 3): the Davoei, Margaritatus, and Spinatum zones. This scheme was also adopted by Fantasia et al. (2018), who additionally studied the nannofossil biostratigraphy of the same section. These studies were the foundation to assign Bed 2-1 to the upper Davoei to lower Margaritatus Zone and Bed 2-2 to the Margaritatus Zone (for sections with bed numbers see chapter 5). Based on the stratigraphic correlation by Aberhan (1992), Beds 6-7, 6-8, and 6-9 should be slightly younger than Beds 2-1 and 2-2. Consequently, they can be assigned to the Spinatum Zone.

Toarcian oyster shells and one brachiopod were available from sections 4, 5, and 6 near El Transito. Beds 4-1, 5-7, and 6-10 correspond to a conspicuous oolitic ironstone to bioclastic limestone unit almost directly above a thick package of sandstones. This stratigraphic interval has been assigned to the Upper Toarcian Copiapense and Tenuicostatum zones (not to be confused with the European Lower Toarcian Tenuicostatum Zone;

compare von Hillebrandt 1973, 1987; Aberhan and von Hillebrandt 1996), which are equivalent to the Thouarsense and lowermost Levesquei zones of Europe (e.g., Pérez et al. 2008). The overlying marly limestones with Beds 4-2 and 4-3 have been assigned to the Lotharingica and Fluitans zones (compare Aberhan and von Hillebrandt 1996), which are equivalent to the middle and upper Levesquei Zone of Europe (e.g., Pérez et al. 2008).

3 Material and methods

Fifty-nine shells of oysters and brachiopods from the Lower Jurassic strata of northern Chile were used in the current study. The fossil material was originally collected by Martin Aberhan for a palaeoecological study (Aberhan 1992, 1993) and is now stored in the collections of the Bayerische Staatssammlung für Paläontologie und Geologie in Munich, Germany. The diverse benthic fauna has been identified and described in detail by Aberhan (1992) and contains a number of species with an original calcitic shell enabling stable isotope analyses. Taxa used in the present study include oysters of the genera *Gryphaea* and *Actinostreon* as well as rhynchonellid brachiopods of the genera *Gibbirhynchia*, *Tetrarhynchia*, *Quadratirhynchia*, *Rudirhynchia*, and *Rhynchonelloidea*. One specimen of the spiriferid brachiopod *Spiriferina chilensis* was analyzed as well. Illustrations of these taxa can be found in taxonomic studies (e.g., Manceñido 1981; Manceñido and Dagys 1992; Aberhan 1994; Baeza-Carratalá 2013).

All specimens were checked for diagenetic alteration before analyzing their stable isotope ($\delta^{13}C$, $\delta^{18}O$) composition. Sections of 5–10 mm thickness were cut through the shells and their surface ground (Fig. 2a, b). All specimens were then studied with a cold cathodoluminescence microscope at the GeoZentrum Nordbayern of the Friedrich-Alexander-Universität Erlangen-Nürnberg, Germany. Non-luminescent areas were selected for sampling, while specimens with a very thin or luminescent shell were excluded from the collection. Few carbonate samples of presumably altered shells, sediment, and sparitic cement filling shells were measured for comparison purposes. Furthermore, three large oyster shells of the genus *Gryphaea* were selected for high-resolution stable isotope analyses (Fig. 2c–e). Results of these three shells were used for seasonality reconstructions and listed as well as interpreted separately. Carbonate samples were taken with a hand-held dental drill in the case of thick shells or with a computer-controlled micromill at the GeoZentrum Nordbayern. In summary, the isotopic composition of 105 brachiopod and oyster samples was analyzed using a carbonate preparation device (Kiel IV) connected with a ThermoScientific MAT 253 mass spectrometer at the Leibniz Laboratory for Radiometric Dating and Stable Isotope Research at the Christian-Albrechts-Universität zu Kiel, Germany. The carbonate samples were reacted within the preparation device with 100% orthophosphoric acid at 75 °C and the evolved CO_2 gas was analyzed using the mass spectrometer. On daily routine, different laboratory internal carbonate standards and two international carbonate standards (NBS-19; IAEA-603) were analyzed to control the precision of measured $\delta^{13}C$ and $\delta^{18}O$ values. All values are reported in per mil relative to the Vienna Pee Dee Belemnite (VPDB) scale using NBS-19. Generally, one sample was collected from each fossil shell and analyzed, but in the case of the three oysters used for high-resolution analyses between 16 to 21 samples were collected. Ten brachiopod shells, which were believed to be well preserved, did not yield enough carbonate powder for stable isotope analyses, because their shells were too thin. For the resulting $\delta^{18}O$ values of well-preserved shells, palaeotemperatures were calculated using the equation given by Anderson and Arthur (1983) with a $\delta^{18}O$ value of -1‰ VSMOW for seawater during shell precipitation (as suggested for an ice-free Jurassic world; Shackleton and Kennett 1975).

4 Preservation of the fossil material

Calcareous shells of marine organisms can store information on sea water temperatures in Earth's history as shown by a large number of geochemical studies (e.g., Epstein et al. 1951; Urey et al. 1951). However, the chemical composition of shells can change after the death of the animal, for example, when pore fluids enter the shells along fractures. It is therefore very important in any such study to carefully examine the preservation of the fossil material used. Consequently, cathodoluminescence microscopy has become a standard procedure for stable isotope research on fossil shells (e.g., Wierzbowski 2002, 2004; Wierzbowski and Joachimski 2007; Ullmann and Korte 2015; Arabas 2016). Most shells in the present study revealed a good preservation with largely dark and non-luminescent shells (Fig. 3a). Only some shells showed a red to orange luminescence thought to be caused by Mn^{2+} which entered the calcite after the burial of the shell (e.g., Fürsich et al. 2005; Wierzbowski et al. 2009; also compare Barbin 2013). In the present cases, these alterations were strongest along fractures, which might have served as pathways for fluids entering the shells (Fig. 3b). Only specimens with large non-luminescent areas, believed to be well-preserved, were used for oxygen isotope analyses and temperature reconstructions, while some altered shells were analyzed for comparison purposes. Cathodoluminescence microscopy led to an exclusion of 15 specimens from the total collection of 59 shells.

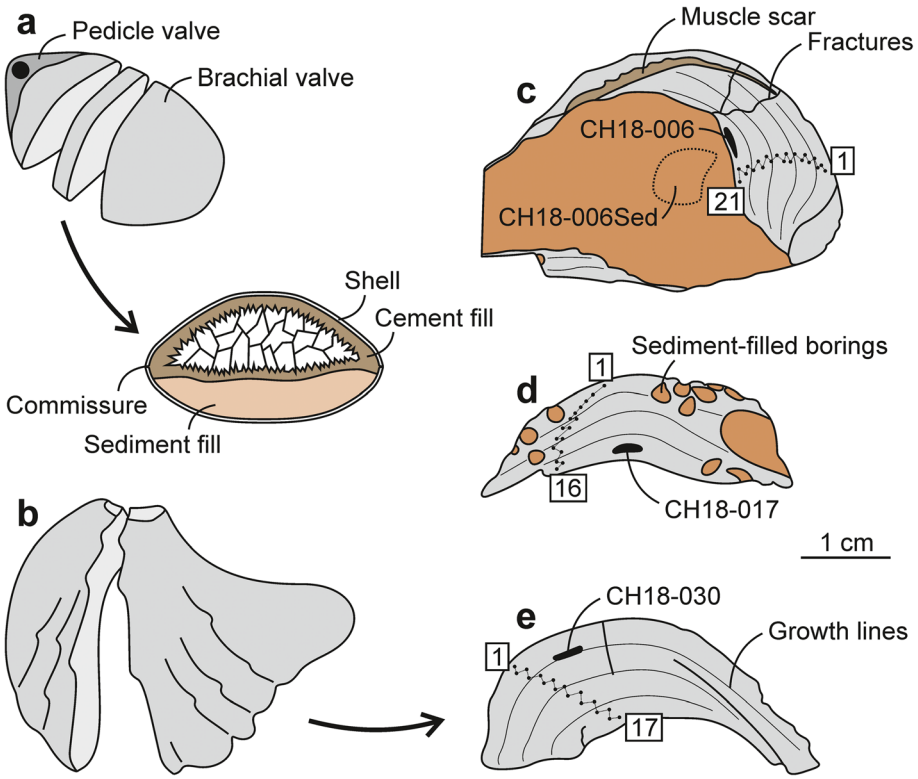

Fig. 2 Preparation of the fossil material (modified after Alberti et al. 2012a, 2012b, 2017, 2019). **a**, **b** Sections of 5–10 mm thickness were cut from each shell and studied with a cathodoluminescence microscope to select sample areas; **c**–**e** Three oyster specimens (CH18-006, CH18-017, and CH18-030) were used for high-resolution stable isotope analyses

Another possible indicator for alteration is a correlation between the $\delta^{18}O$ and $\delta^{13}C$ values of the analyzed shells. Sedimentary rocks are commonly characterized by lower $\delta^{18}O$ and $\delta^{13}C$ values than fossil shells, especially after diagenetic alteration or influence by meteoric waters (e.g., Hodgson 1966; Hudson 1977; Nelson and Smith 1996). Similarly, stable isotope ratios of fossil shells shift towards lower values with increasing alteration leading to a correlation between both values in the dataset. Such a correlation should therefore be treated with caution, although in some cases it can be primary in origin, for example, because of an increase in primary productivity with higher water temperatures.

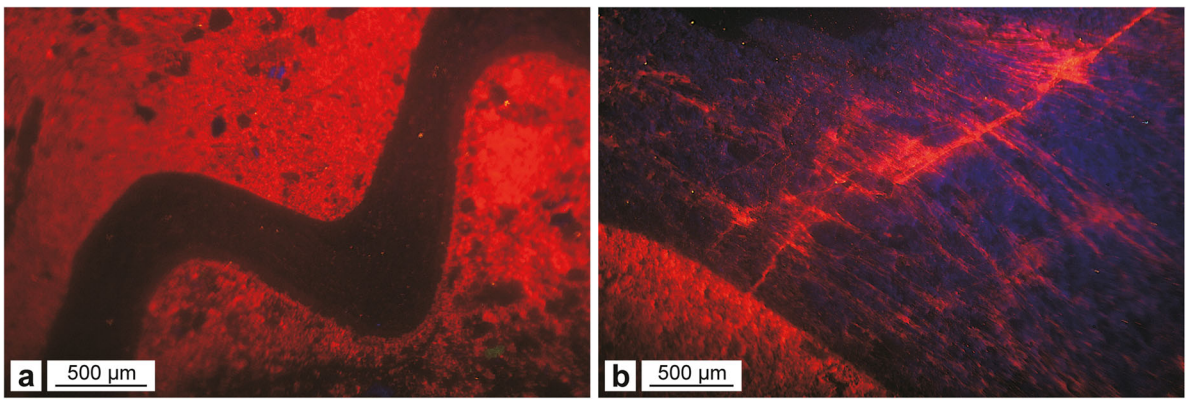

Fig. 3 Cathodoluminescence microscopy. **a** Well-preserved shell of *Rudirhynchia* aff. *rudis* from the Upper Pliensbachian (CH18-001); **b** Poorly preserved shell of *Gryphaea* cf. *dumortieri* from the Upper Pliensbachian (CH18-050)

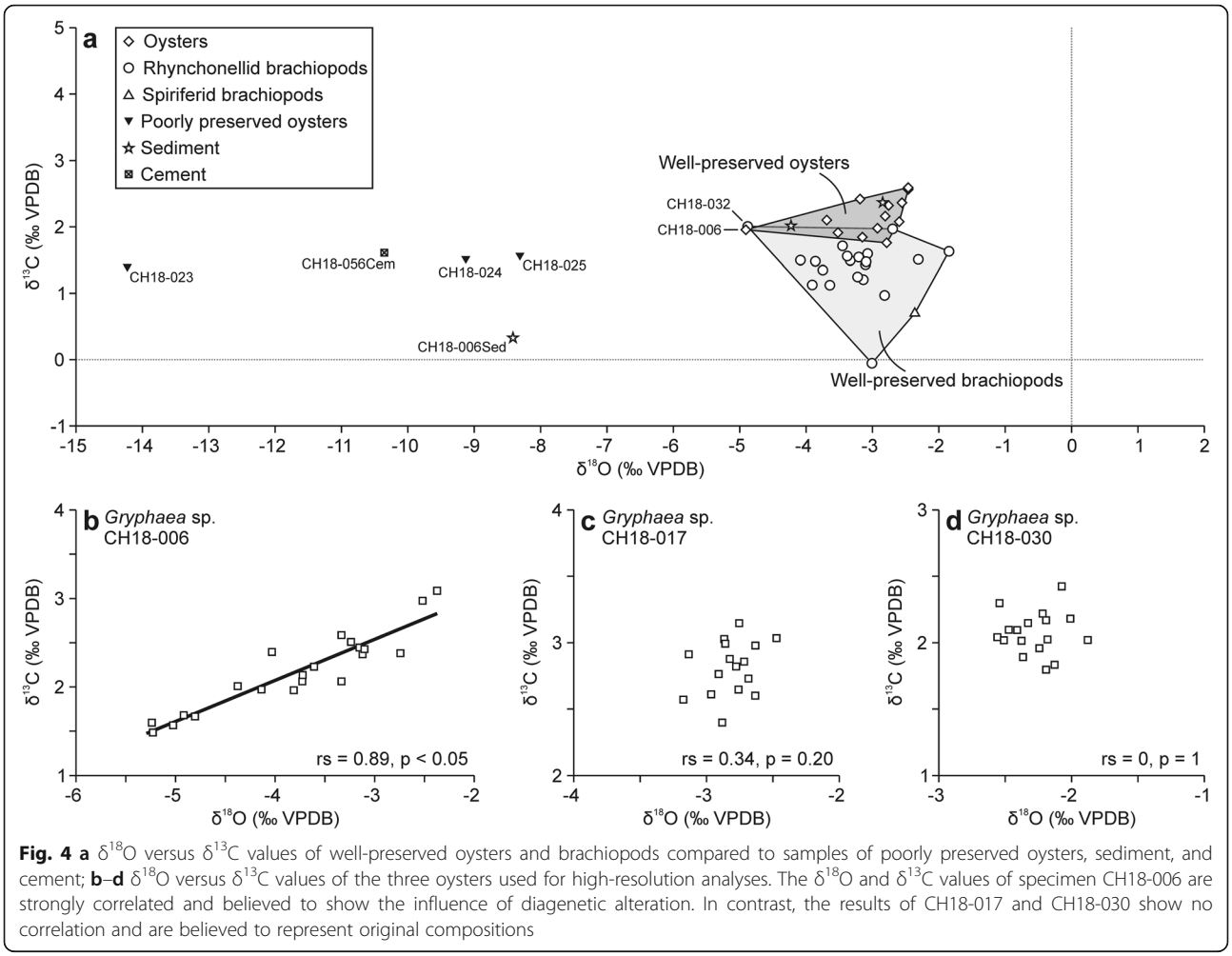

Fig. 4 **a** $\delta^{18}O$ versus $\delta^{13}C$ values of well-preserved oysters and brachiopods compared to samples of poorly preserved oysters, sediment, and cement; **b**–**d** $\delta^{18}O$ versus $\delta^{13}C$ values of the three oysters used for high-resolution analyses. The $\delta^{18}O$ and $\delta^{13}C$ values of specimen CH18-006 are strongly correlated and believed to show the influence of diagenetic alteration. In contrast, the results of CH18-017 and CH18-030 show no correlation and are believed to represent original compositions

The present dataset of stable isotope ($\delta^{18}O$, $\delta^{13}C$) values of well-preserved oyster and brachiopod shells as well as of altered oysters, sediment, and cement samples is illustrated in Fig. 4a. While the $\delta^{13}C$ values of the individual samples are comparatively similar, the $\delta^{18}O$ values range widely. In particular, the samples of poorly preserved oysters and cement show very low $\delta^{18}O$ values (less than -8‰). The Spearman correlation coefficient indicates no significant correlation between $\delta^{18}O$ and $\delta^{13}C$ values of the well-preserved brachiopods ($rs = -0.08$; $p = 0.74$). The values of seemingly well-preserved oyster shells are moderately correlated ($rs = 0.56$; $p = 0.05$). This correlation is mainly due to specimen CH18–006 with a comparatively low $\delta^{18}O$ value. If this sample is excluded from the dataset, the correlation is statistically not significant with a p-value above 5%.

Three oysters were selected for high-resolution stable isotope analyses (Fig. 2c–e). The data of specimen CH18–006 show a strong correlation between $\delta^{18}O$ and $\delta^{13}C$ values (Fig. 4b; $rs = 0.89$; $p < 0.05$), which is believed to be due to the influence of diagenetic alteration. Results of this specimen were therefore not used for temperature reconstructions. Stable isotope data of the other two specimens CH18-017 and CH18-030 show no significant correlation (Fig. 4c, d) and are therefore believed to represent original conditions.

In summary, cathodoluminescence microscopy and the evaluation of a potential correlation between $\delta^{18}O$ and $\delta^{13}C$ values indicate a good preservation of the shells used for temperature reconstructions (except for specimen CH18-006).

5 Results of the stable isotope analyses

The results of the stable isotope ($\delta^{13}C$, $\delta^{18}O$) analyses of well-preserved oysters and brachiopods are listed in Table 1. In addition, Table 1 lists the data from poorly preserved oysters, sediment and cement samples. The data obtained from high-resolution analyses of the three oyster shells can be found in Table 2.

Figure 5 illustrates the stratigraphic position of the sampled shells and shows the $\delta^{13}C$ and $\delta^{18}O$ values of the well-preserved oysters and brachiopods. While the data for the Sinemurian and Pliensbachian are retrieved

Table 1 Results of the stable isotope ($\delta^{13}C$, $\delta^{18}O$) analyses of oysters and brachiopods from the Lower Jurassic of northern Chile. In addition to well-preserved shells, some luminescent and altered oyster shells as well as sediment and cement samples were analyzed. Please note that the high-resolution analysis of specimen CH18-006 indicated a diagenetic alteration of this shell, which has consequently not been used for further interpretations

Specimen no.	Taxonomy	Bed no.	Age	Ammonite zone	$\delta^{13}C$ (‰ VPDB)	$\delta^{18}O$ (‰ VPDB)	T (°C)[a]
Oysters and brachiopods							
CH18-026	*Actinostreon solitarium*	4-3	Late Toarcian	Middle to upper Levesquei	2.57	-2.46	22.3
CH18-027	*Actinostreon solitarium*	4-3	Late Toarcian	Middle to upper Levesquei	1.98	-2.93	24.5
CH18-013	*Actinostreon solitarium*	4-2	Late Toarcian	Middle to upper Levesquei	2.08	-2.60	22.9
CH18-014	*Actinostreon solitarium*	4-2	Late Toarcian	Middle to upper Levesquei	1.84	-3.15	25.5
CH18-006	*Gryphaea* sp.	6-10	Late Toarcian	Thouarsense – lower Levesquei	1.96	-4.91	(34.2)
CH18-007	*Gryphaea* sp.	6-10	Late Toarcian	Thouarsense – lower Levesquei	1.91	-3.52	27.3
CH18-008	*Gryphaea* sp.	6-10	Late Toarcian	Thouarsense – lower Levesquei	2.10	-3.69	28.1
CH18-015	*Gryphaea* sp.	5-7	Late Toarcian	Thouarsense – lower Levesquei	2.59	-2.46	22.3
CH18-016	*Gryphaea* sp.	5-7	Late Toarcian	Thouarsense – lower Levesquei	2.32	-2.76	23.7
CH18-017	*Gryphaea* sp.	5-7	Late Toarcian	Thouarsense – lower Levesquei	2.42	-3.19	25.7
CH18-029	*Gryphaea* sp.	4-1	Late Toarcian	Thouarsense – lower Levesquei	2.16	-2.81	23.9
CH18-030	*Gryphaea* sp.	4-1	Late Toarcian	Thouarsense – lower Levesquei	1.76	-2.79	23.8
CH18-046	*Rhynchonelloidea* sp.	4-1	Late Toarcian	Thouarsense – lower Levesquei	-0.05	-3.01	24.8
CH18-048	*Actinostreon solitarium*	4-1	Late Toarcian	Thouarsense – lower Levesquei	2.36	-2.56	22.8
CH18-002	*Rudirhynchia* aff. *rudis*	6-9	Late Pliensbachian	Spinatum	1.63	-1.85	19.6
CH18-001	*Rudirhynchia* aff. *rudis*	6-8	Late Pliensbachian	Spinatum	1.60	-3.07	25.1
CH18-032	*Tetrarhynchia tetraheda*	2-2	Late Pliensbachian	Margaritatus	2.01	-4.88	34.0
CH18-034	*Quadratirhynchia lenticulata*	2-1	Early–Late Pliensbachian	Upper Davoei – lower Margaritatus	1.48	-3.86	28.9
CH18-003	*Spiriferina chilensis*	5-4	Late Sinemurian	Raricostatum	0.72	-2.36	21.9
CH18-056	*Gibbirhynchia curviceps*	6-6	Late Sinemurian	Raricostatum	1.51	-2.31	21.6
CH18-057	*Gibbirhynchia curviceps*	6-6	Late Sinemurian	Raricostatum	1.25	-3.22	25.9
CH18-059	*Gibbirhynchia curviceps*	6-6	Late Sinemurian	Raricostatum	1.71	-3.45	26.9
CH18-037	*Gibbirhynchia curviceps*	5-3	Late Sinemurian	Raricostatum	1.97	-2.70	23.4
CH18-038	*Gibbirhynchia curviceps*	5-3	Late Sinemurian	Raricostatum	1.21	-3.14	25.4
CH18-040	*Gibbirhynchia curviceps*	5-3	Late Sinemurian	Raricostatum	1.48	-3.10	25.2
CH18-018	*Gibbirhynchia curviceps*	6-5	Late Sinemurian	Raricostatum	1.12	-3.64	27.8
CH18-019	*Gibbirhynchia curviceps*	6-5	Late Sinemurian	Raricostatum	1.50	-4.09	30.0
CH18-043	*Quadratirhynchia crassimedia*	6-5	Late Sinemurian	Raricostatum	0.97	-2.82	24.0
CH18-045	*Quadratirhynchia crassimedia*	6-5	Late Sinemurian	Raricostatum	1.56	-3.38	26.6
CH18-021	*Quadratirhynchia crassimedia*	6-3	Late Sinemurian	Raricostatum	1.55	-3.21	25.8
CH18-052	*Gibbirhynchia* cf. *curviceps*	5-2	Late Sinemurian	Raricostatum	1.43	-3.11	25.3
CH18-054	*Quadratirhynchia crassimedia*	5-1	Late Sinemurian	Raricostatum	1.13	-3.91	29.1
CH18-055	*Quadratirhynchia crassimedia*	5-1	Late Sinemurian	Raricostatum	1.35	-3.75	28.4
CH18-010	*Quadratirhynchia crassimedia*	6-1	Late Sinemurian	Raricostatum	1.49	-3.34	26.4
Luminescent, altered shells							
CH18-023	*Gryphaea tricarinata*	–	Late Sinemurian	–	1.39	-14.23	(93.5)

Table 1 Results of the stable isotope ($\delta^{13}C$, $\delta^{18}O$) analyses of oysters and brachiopods from the Lower Jurassic of northern Chile. In addition to well-preserved shells, some luminescent and altered oyster shells as well as sediment and cement samples were analyzed. Please note that the high-resolution analysis of specimen CH18-006 indicated a diagenetic alteration of this shell, which has consequently not been used for further interpretations *(Continued)*

Specimen no.	Taxonomy	Bed no.	Age	Ammonite zone	$\delta^{13}C$ (‰ VPDB)	$\delta^{18}O$ (‰ VPDB)	T (°C)[a]
CH18-024	*Gryphaea tricarinata*	–	Late Sinemurian	–	1.51	-9.13	(58.2)
CH18-025	*Gryphaea tricarinata*	–	Late Sinemurian	–	1.56	-8.31	(53.2)
Sediment and cement samples							
CH18-006Sed	Sediment fill	6-10	Late Toarcian	Thouarsense – lower Levesquei	0.33	-8.42	(53.9)
CH18-022Sed	Sediment fill	6-2	Late Sinemurian	Raricostatum	2.02	-4.23	(30.7)
CH18-038Sed	Sediment fill	5-3	Late Sinemurian	Raricostatum	2.37	-2.85	(24.1)
CH18-056Cem	Cement fill	6-6	Late Sinemurian	Raricostatum	1.61	-10.36	(66.1)

[a]Temperatures are calculated with the equation of Anderson and Arthur (1983) and a $\delta^{18}O$ value of -1‰ VSMOW for seawater during shell formation (Shackleton and Kennett 1975)

from brachiopods, the Toarcian is mostly represented by oyster shells. The $\delta^{13}C$ values show an overall slight increase from the Sinemurian to the Toarcian. They fluctuate around an average of 1.37‰ in the Upper Sinemurian (range: 0.72‰ to 1.97‰). Although the data for the Pliensbachian is limited, $\delta^{13}C$ values seem to be higher around an average of 1.68‰ (range: 1.48‰ to 2.01‰). Apart from one outlier (specimen CH18-046: -0.05‰), the highest $\delta^{13}C$ values have been recorded in the upper Toarcian with an average of 2.00‰ (range: 1.76‰ to 2.59‰).

The $\delta^{18}O$ values show some fluctuations through time. In the late Sinemurian, the values range around an average of -3.22‰ (range: -4.09‰ to -2.31‰) with the highest values close to the Sinemurian–Pliensbachian boundary (Fig. 5). In the Pliensbachian, there are two outliers with comparatively low values (CH18-032: -4.88‰; CH18-034: -3.86‰). These two shells (which show $\delta^{13}C$ values similar to the other shells) are from section 2 near Potrerillos around 280 km north of all other analyzed shells (Fig. 1). The other two Pliensbachian shells from a higher stratigraphic interval near the boundary to the Toarcian show comparatively high $\delta^{18}O$ values around an average of -2.46‰ (CH18-001: -3.07‰; CH18-002: -1.85‰). In the late Toarcian, the data fluctuate around an average of -2.92‰ (range: -3.69‰ to -2.46‰). This interval also contains specimen CH18-006, which has been excluded from interpretation, as it has shown signs of diagenetic alteration during high-resolution analysis (see above).

In summary, the $\delta^{13}C$ and $\delta^{18}O$ values show differing trends through time. While the $\delta^{13}C$ values show an overall steady increase through time, the changes in the $\delta^{18}O$ values are somewhat more complex. Over most of the late Sinemurian, the $\delta^{18}O$ values are below -3‰. Just below the Sinemurian–Pliensbachian boundary, the average $\delta^{18}O$ value rises above -3‰. The highest $\delta^{18}O$ value in the entire dataset is reached at the end of the Pliensbachian. The $\delta^{18}O$ values in the late Toarcian are again lower but not as low as in the late Sinemurian (Fig. 5).

The results of the three oysters used for high-resolution stable isotope analyses are shown in Fig. 6. As described already above, the $\delta^{13}C$ and $\delta^{18}O$ values of specimen CH18-006 are correlated strongly (Fig. 6a). Throughout the shell, the $\delta^{18}O$ values decrease to lower values with a few fluctuations. This pattern is almost perfectly mirrored in the $\delta^{13}C$ values. These parallel trends are believed to be caused by diagenetic alteration and specimen CH18-006 was excluded from further interpretation. In contrast, the $\delta^{13}C$ and $\delta^{18}O$ values of the oysters CH18-017 and CH18-030 indicate an original stable isotope composition. Both shells show cyclic patterns in their $\delta^{18}O$ values, while the $\delta^{13}C$ values show very little and unrelated fluctuations (Fig. 6b, c). The $\delta^{18}O$ values of specimen CH18-017 vary around an average of -2.82‰ (range: -3.18‰ to -2.47‰). The data show two minima and three maxima. The $\delta^{18}O$ values of specimen CH18-030 show a somewhat similar pattern, but are slightly higher with an average of -2.28‰ (range: -2.56‰ to -1.88‰). The cycles are less clear compared to CH18-017, but three minima and two maxima can be discerned (most easily by using a two-point running average).

6 Discussion

6.1 Palaeoenvironment

Aberhan (1992) assigned three different depositional environments to the Lower Jurassic strata of the study area: (1) a coastal zone dominated by siliciclastic

Table 2 Results of the high-resolution stable isotope ($\delta^{13}C$, $\delta^{18}O$) analyses of three oysters with a late Toarcian age

Sample no.	$\delta^{13}C$ (‰ VPDB)	$\delta^{18}O$ (‰ VPDB)	T (°C)[a]
Gryphaea sp. (CH18-006; late Toarcian; Bed 6-10)			
CH18-6-1	2.43	-3.10	25.3
CH18-6-2	2.51	-3.24	25.9
CH18-6-3	2.37	-3.12	25.4
CH18-6-4	2.45	-3.15	25.5
CH18-6-5	3.09	-2.37	21.9
CH18-6-6	2.98	-2.52	22.6
CH18-6-7	2.38	-2.74	23.6
CH18-6-8	1.96	-3.81	28.7
CH18-6-9	2.01	-4.38	31.5
CH18-6-10	2.23	-3.61	27.7
CH18-6-11	2.14	-3.72	28.2
CH18-6-12	2.06	-3.73	28.3
CH18-6-13	1.97	-4.14	30.3
CH18-6-14	2.59	-3.33	26.4
CH18-6-15	2.40	-4.03	29.7
CH18-6-16	2.06	-3.33	26.4
CH18-6-17	1.67	-4.81	33.6
CH18-6-18	1.68	-4.92	34.2
CH18-6-19	1.57	-5.03	34.8
CH18-6-20	1.60	-5.24	35.9
CH18-6-21	1.48	-5.23	35.8
Gryphaea sp. (CH18-017; late Toarcian; Bed 5-7)			
CH18-17-1	2.99	-2.86	24.1
CH18-17-2	2.73	-2.68	23.3
CH18-17-3	2.86	-2.72	23.5
CH18-17-4	2.82	-2.78	23.8
CH18-17-5	3.04	-2.47	22.4
CH18-17-6	2.98	-2.63	23.1
CH18-17-7	3.15	-2.75	23.7
CH18-17-8	3.03	-2.87	24.2
CH18-17-9	2.91	-3.13	25.4
CH18-17-10	2.88	-2.83	24.0
CH18-17-11	2.60	-2.63	23.1
CH18-17-12	2.40	-2.88	24.3
CH18-17-13	2.61	-2.97	24.6
CH18-17-14	2.57	-3.18	25.6
CH18-17-15	2.65	-2.76	23.7
CH18-17-16	2.76	-2.91	24.4
Gryphaea sp. (CH18-030; late Toarcian; Bed 4-1)			
CH18-30-1	2.17	-2.19	21.1
CH18-30-2	2.30	-2.54	22.7
CH18-30-3	2.15	-2.33	21.7
CH18-30-4	2.22	-2.22	21.2
CH18-30-5	2.18	-2.01	20.3
CH18-30-6	2.02	-2.38	21.9
CH18-30-7	2.42	-2.07	20.6
CH18-30-8	2.10	-2.47	22.4
CH18-30-9	2.10	-2.41	22.1
CH18-30-10	2.02	-2.51	22.5
CH18-30-11	2.03	-2.18	21.1
CH18-30-12	1.96	-2.24	21.3
CH18-30-13	2.02	-1.88	19.7
CH18-30-14	1.80	-2.19	21.1
CH18-30-15	2.04	-2.56	22.8
CH18-30-16	1.83	-2.13	20.8
CH18-30-17	1.89	-2.37	21.9

[a]Temperatures are calculated with the equation of Anderson and Arthur (1983) and a $\delta^{18}O$ value of -1‰ VSMOW for seawater during shell formation (Shackleton and Kennett 1975)

sediments with sedimentary structures pointing to a setting above or just below the fair-weather wave-base (mainly sand- or siltstones), (2) an intermediate zone dominated by carbonates, but still showing a considerable clay and silt content (mainly bioclastic wacke- to packstones), and (3) a distal zone with low sedimentation rates characterized by very fine-grained terrigenous siliciclastics and carbonate mud (mainly mud- to wackestones and marl). While zones 1 and 2 have comparatively high faunal diversities, zone 3 is characterized by very low diversities (possibly caused by low oxygen availability and soupy substrates; Aberhan 1992).

Shells used in the present study are from the deeper part of zone 1 and zone 2 (compare Fig. 5). Some shells come from siltstones or mixed carbonate–siliciclastics (partly with ferruginous ooids), which represent somewhat deeper water around or just below the fair-weather wave-base (zone 1 of Aberhan 1992). Most fossils come from carbonates (zone 2 of Aberhan 1992), which are occasionally marly or are developed as shell beds possibly formed by storm action (the repeated occurrence of higher energy conditions such as storms has also been suggested by Fantasia et al. 2018). No direct correlation between the results of the stable isotope analyses and the facies types (= water depth) can be seen (Fig. 5) and it can be assumed that the analyzed shells were formed above the thermocline and therefore represent sea-surface water conditions.

Apart from the water temperature, the stable isotope ($\delta^{18}O$) composition of shells in marine environments

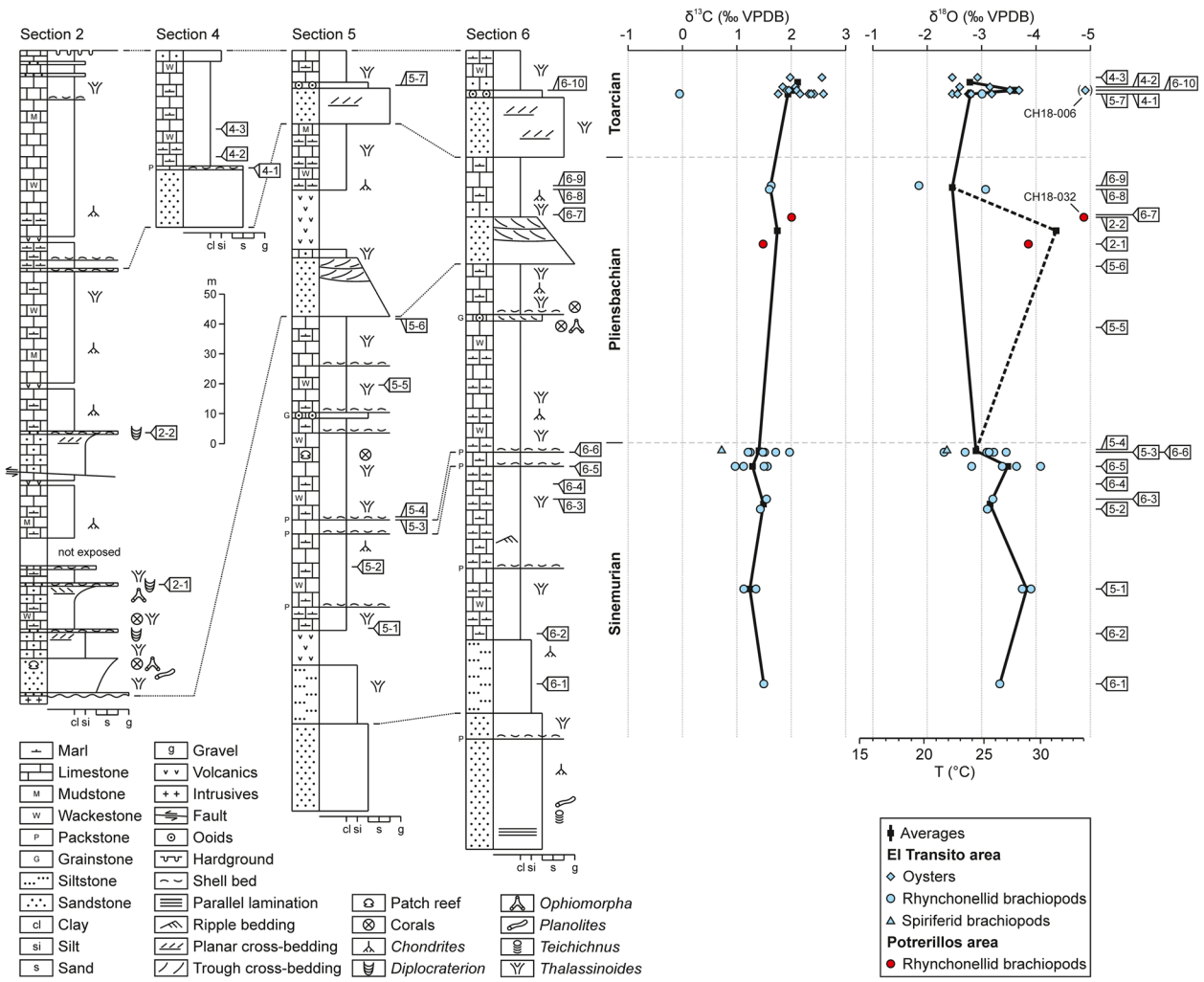

Fig. 5 Lithologs (modified after Aberhan 1992) with the position of the individual samples and the results of the stable isotope ($\delta^{13}C$, $\delta^{18}O$) analyses of well-preserved oysters and brachiopods. Note the inverted scale for $\delta^{18}O$ values

can be influenced by salinity fluctuations. A deviation from the normal marine salinity due to freshwater influx (rain fall or river discharge) or strong evaporation (e.g., in an enclosed lagoon) can considerably alter the oxygen isotope composition of the ocean water and consequently of the shells. As described above, the fossil material used in the present study represents a shallow water depth slightly above the fair-weather wave-base or just below, but still above the thermocline and within reach of occasional stronger storms. No fossils have been used from the cross-bedded sandstones which formed in a very shallow setting. Freshwater influx via stronger rain fall affecting the uppermost water layers can therefore be excluded. Strong deviations from normal marine salinity are also unlikely considering that the fossils collected in the stratigraphic interval studied include stenohaline forms such as corals, brachiopods, crinoids, and ammonites (Fig. 5; Aberhan 1992; compare also Fantasia et al. 2018).

6.2 Carbon isotope record

The $\delta^{13}C$ data (Fig. 5) indicate a trend towards higher values, however, it should be noted that the Sinemurian and Pliensbachian samples are represented by brachiopods, while the Toarcian data come mainly from oysters. The $\delta^{13}C$ values of oysters are consistently higher than those of the brachiopods (Fig. 4a), even though the $\delta^{18}O$ values are comparable. Vital effects causing higher $\delta^{13}C$ values of oysters might therefore explain the recorded "trend" from the Sinemurian to the Toarcian at least in parts. This is in broad agreement with the dataset of Korte et al. (2015) for the Early Jurassic, which shows mostly higher $\delta^{13}C$ values in bivalves than in brachiopods of the same age. Other studies, however, show that co-occurring bivalves and

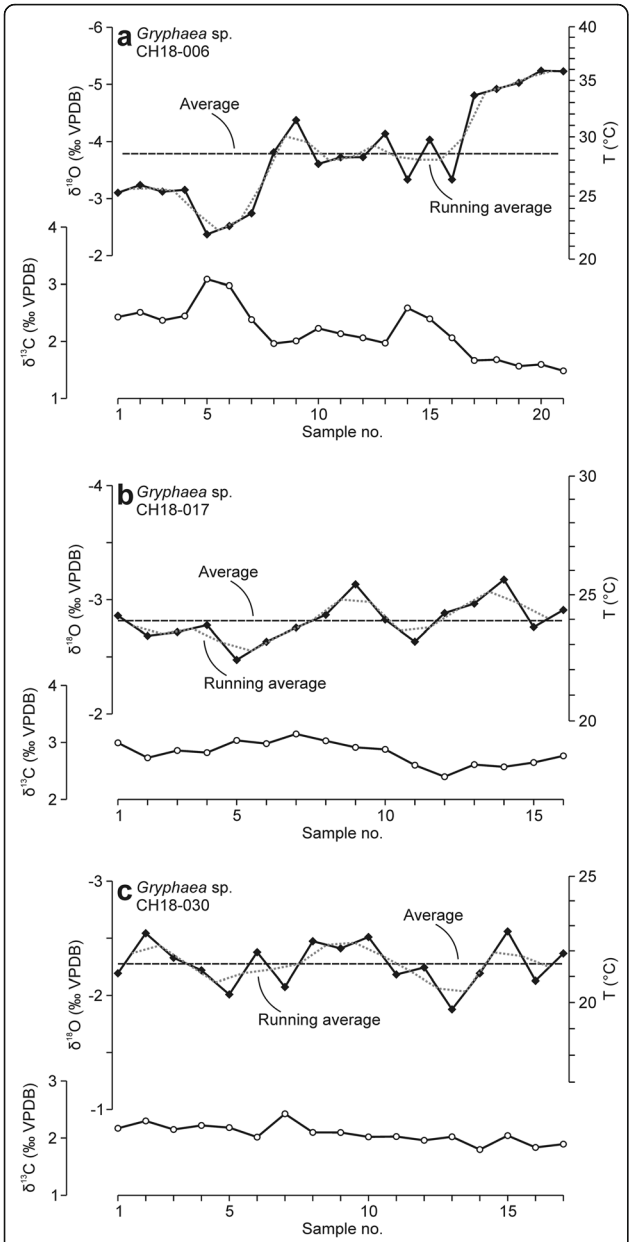

Fig. 6 Results of the high-resolution stable isotope ($\delta^{13}C$, $\delta^{18}O$) analyses of three oysters with a late Toarcian age. While the data of specimen CH18-006 (**a**) shows evidence of diagenetic alteration, the values of CH18-017 (**b**) and CH18-030 (**c**) are assumed to reflect original conditions representing seasonal temperature fluctuations. In addition to the overall average for each dataset, a two-point running average is shown. Note the inverted scale for $\delta^{18}O$ values

brachiopods have very similar $\delta^{13}C$ values (e.g., Alberti et al. 2017, 2019). Further data of different faunal groups is therefore necessary to judge whether there actually is a trend in the $\delta^{13}C$ values through time or whether the difference is merely caused by vital effects. Apart from this problem, the absolute $\delta^{13}C$ values are comparable to those of shells from Europe (e.g., Korte et al. 2015).

Lower Jurassic rocks include a number of prominent carbon isotope excursions including one during the Toarcian Oceanic Anoxic Event (e.g., Jenkyns 1988; Hesselbo et al. 2000a, 2007; Pálfy and Smith 2000; van de Schootbrugge et al. 2005a; Gómez et al. 2008; Suan et al. 2008, 2011; Littler et al. 2010; Korte and Hesselbo 2011; Silva et al. 2011; Caswell and Coe 2012; Riding et al. 2013; Kemp and Izumi 2014; Krencker et al. 2014; Ait-Itto et al. 2017; Arabas et al. 2017; Bougeault et al. 2017; Menini et al. 2019; Mercuzot et al. 2019). The TOAE has also been reported from Argentina (Al-Suwaidi et al. 2010, 2014, 2016; Mazzini et al. 2010) and Chile (Fantasia et al. 2018). Fantasia et al. (2018) reported several negative carbon isotope excursions based on analyses of whole-rock samples (i.e. within the Margaritatus Zone, at the Pliensbachian–Toarcian boundary, and during the TOAE). These excursions are not visible in the present $\delta^{13}C$ values of fossil shells (Fig. 5), because they were of relatively short duration and/or the stratigraphic intervals where they are most pronounced are not represented by fossils (compare Boulila and Hinnov 2017). The variation in the $\delta^{13}C$ values of fossil shells is relatively small compared to that recorded by Fantasia et al. (2018) from whole-rock analyses. The only exception is specimen CH18-046 from the upper Toarcian, which shows a much lower $\delta^{13}C$ value than all other shells analyzed. However, this shell has a considerably younger age than the previously reported negative carbon isotope excursions, and since other shells from the same horizon show higher values, it might be less reliable. It can be therefore presumed that the presented dataset represents background conditions prevalent over most of the Early Jurassic and not exceptional events.

6.3 Water temperatures

Considering that the shells formed above the thermocline and in normal marine salinity conditions, the recorded $\delta^{18}O$ values can be translated into sea-surface water-temperatures. In accordance with the majority of other studies on Jurassic stable isotopes, the equation of Anderson and Arthur (1983) with a $\delta^{18}O$ value of -1‰ VSMOW for seawater during shell precipitation (as suggested for an ice-free Jurassic world; Shackleton and Kennett 1975) was used. The reconstructed water temperatures show several fluctuations through time (Fig. 5). During most of the late Sinemurian, temperatures were relatively high (average: 27.0 °C). Just before the Sinemurian–Pliensbachian transition, temperatures dropped to an average of 24.3 °C. At the Quebrada El Asiento (section 2) near Potrerillos, the results point to very warm conditions during the Pliensbachian (average: 31.4 °C). Further south near El Transito (sections 4, 5, 6) temperatures were much lower (average: 22.3 °C). The lowest temperature in the entire dataset was recorded for the latest Pliensbachian (specimen CH18-002: 19.6 °C).

No data is available for the early Toarcian, but results indicate again higher temperatures for the late Toarcian (average: 24.4 °C) comparable to those of the late Sinemurian.

The data retrieved by high-resolution stable isotope ($\delta^{18}O$) analyses of the two oysters CH18-017 and CH18-030 can be translated into seasonal temperature fluctuations (Fig. 6b, c). Both shells show similar conditions in the late Toarcian reflecting temperature cycles during a period of around 3 years in the life time of the oysters. If explained only by temperature, the $\delta^{18}O$ values of specimen CH18-017 record an average temperature of 23.9 °C with a minimum of 22.4 °C and a maximum of 25.6 °C. The $\delta^{18}O$ values of specimen CH18-030 record a slightly lower average temperature of 21.5 °C with a minimum of 19.7 °C and a maximum of 22.8 °C. Since the oyster shells are not very large (Fig. 2d, e), the temporal resolution of samples is not very high for both shells with a year being represented by less than ten samples. Therefore true temperature maxima and minima occurring over the life time of the oysters are not recorded. Each value instead represents an average temperature of a period of one to 2 months. The reconstructed seasonality of slightly more than 3 °C for both shells is therefore only a minimum estimate.

6.4 Comparisons with previously published data

So far, reconstructions of absolute seawater temperatures for the Early Jurassic using the stable isotope ($\delta^{18}O$) composition of fossil hard parts are almost completely restricted to European and neighboring localities (e.g., Sælen et al. 1996; Hesselbo et al. 2000b; McArthur et al. 2000, 2007; Bailey et al. 2003; Nori and Lathuilière 2003; Rosales et al. 2004a, 2004b, 2018; van de Schootbrugge et al. 2005b; Gómez et al. 2008, 2016; Metodiev and Koleva-Rekalova 2008; Suan et al. 2008, 2010; Dera et al. 2009a, 2009b, 2011; Gómez and Arias 2010; Price 2010; Korte and Hesselbo 2011; Armendáriz et al. 2012; Li et al. 2012; Harazim et al. 2013; Teichert and Luppold

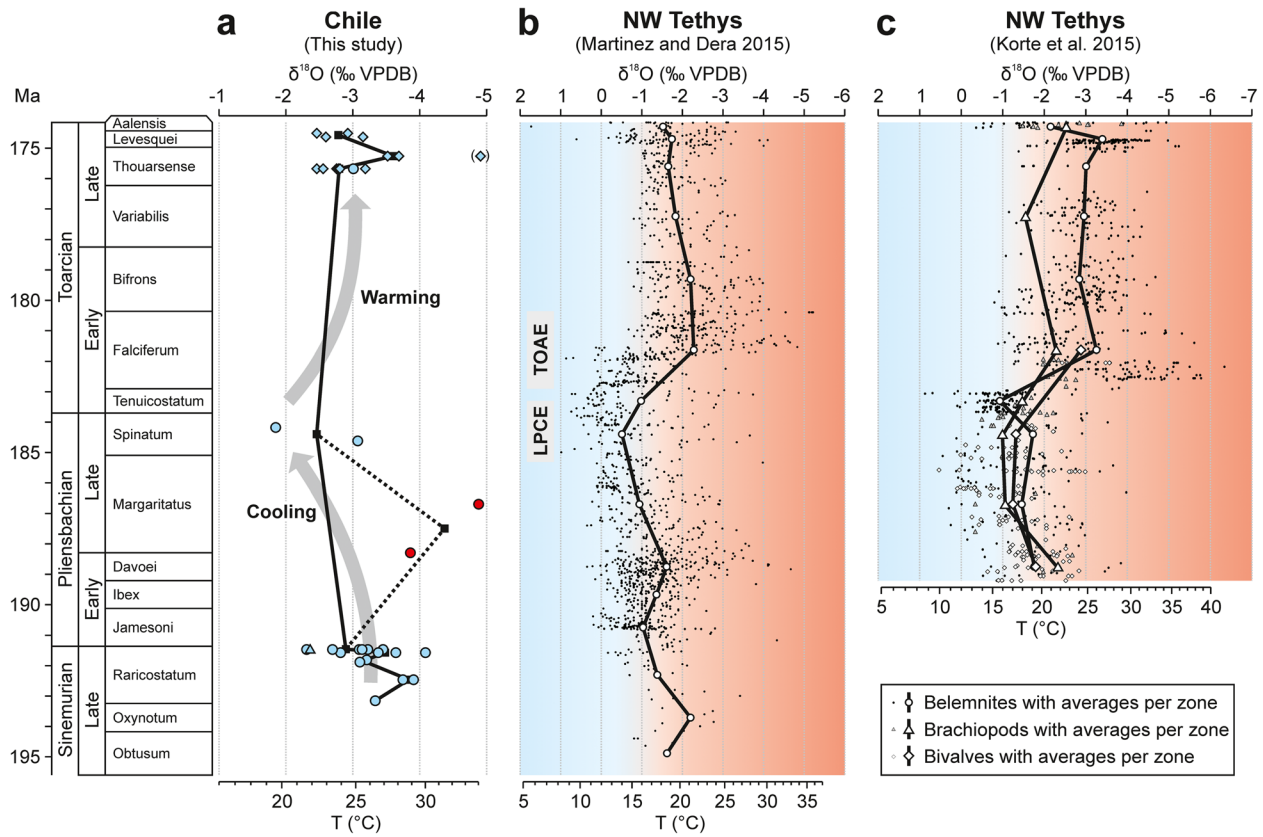

Fig. 7 The Early Jurassic $\delta^{18}O$ data from **a** Chile (for legend see Fig. 5) compared to the large datasets of **b** Martinez and Dera (2015) and **c** Korte et al. (2015) from the northwestern Tethys for the same time interval. The dataset of Martinez and Dera (2015) consists of 1662 individual belemnite samples (from Hesselbo et al. 2000b; McArthur et al. 2000; Jenkyns et al. 2002; Bailey et al. 2003; Gómez et al. 2008; Metodiev and Koleva-Rekalova 2008; Dera et al. 2009b, 2011; Price 2010; Korte and Hesselbo 2011; Armendáriz et al. 2012; Li et al. 2012; Harazim et al. 2013; Riding et al. 2013). The dataset of Korte et al. (2015) consists of 823 individual belemnite samples in addition to the results of 140 bivalves and 46 brachiopods (integrating their new data with that of McArthur et al. 2000; Cresta et al. 2001; Jenkyns et al. 2002; Suan et al. 2008; Price 2010; Korte and Hesselbo 2011; Li et al. 2012; Ullmann et al. 2014). Note the inverted scale for $\delta^{18}O$ values

2013; Krencker et al. 2014, 2015; Metodiev et al. 2014; Korte et al. 2015; Martinez and Dera 2015; Price et al. 2016; Arabas et al. 2017). In these regions of the northwestern Tethys, previously published results show decreasing temperatures from the late Sinemurian throughout the Pliensbachian with a temperature minimum in the late Pliensbachian and around the Pliensbachian–Toarcian boundary. Temperatures then strongly increased in the early Toarcian with the development of the Toarcian Oceanic Anoxic Event, but remained relatively high throughout the Toarcian until they again decreased strongly into the Aalenian (Korte et al. 2015). Even though most authors agree that temperatures increased dramatically throughout the early Toarcian, some authors have questioned the reconstructed amplitude of this change and attributed at least part of it to a parallel change in the $\delta^{18}O$ values of the seawater (e.g., by the disappearance of polar ice shields or an increased freshwater runoff in the Toarcian; Sælen et al. 1996; Rosales et al. 2004b; Suan et al. 2008; Dera et al. 2009b, 2011; Dera and Donnadieu 2012; Korte et al. 2015).

Temperature reconstructions for regions outside Europe especially those based on stable isotope ($\delta^{18}O$) analyses are very scarce (Volkheimer et al. 2008). Bowen (1963) analyzed eight poorly dated belemnites from the Lower Jurassic of Argentina. After dismissing one specimen due to unlikely analytical results, his $\delta^{18}O$ results vary between -0.1‰ and -2.9‰ (equivalent to temperatures of 12.4 °C to 24.3 °C using a $\delta^{18}O$ for seawater of -1‰ and the equation of Anderson and Arthur 1983). Interestingly, Bowen (1963) reconstructed a seasonality of 3.3 °C to 3.7 °C based on his belemnites, which is quite comparable to the results of the present study. However, since his data is only known to be Lower Jurassic, it can hardly be compared to the current dataset considering the likelihood of prominent climate changes during this time interval.

The current study is the first to present Early Jurassic absolute water temperatures from South America based on material which could be assigned to ammonite zones. Figure 7 interprets the presented data from Chile and compares it to the datasets compiled by Martinez and Dera (2015) and Korte et al. (2015) for the northwestern Tethys. Martinez and Dera (2015) and Korte et al. (2015) compiled high-resolution stable isotope ($\delta^{18}O$) records from European localities which show almost identical patterns. The most striking feature is the Late Pliensbachian Cooling Event (LPCE) and the early Toarcian Oceanic Anoxic Event (TOAE). Even though the South American dataset is limited so far, it seems that it broadly follows the temperature pattern already described from Europe. The water temperatures show a general decrease from the late Sinemurian until a minimum in the latest Pliensbachian Spinatum Zone, followed again by a warming until the late Toarcian. Unfortunately, no material from the lower Toarcian was available in the collection to document the possible presence of the early Toarcian warming. The high temperatures at Potrerillos during the Pliensbachian might indicate a special situation in this part of the basin (possibly the influence of freshwater), but more data is needed in order to come to a final conclusion.

On average, the reconstructed absolute water temperatures in Chile are slightly higher than those of the northwestern Tethys (Fig. 7). This can be attributed to a higher palaeolatitude of the European localities in the northern hemisphere compared to Chile in the southern hemisphere. At the same time, it has to be noted that the majority of data from Europe is based on belemnites, which are known to commonly record lower temperatures than co-occurring brachiopods and bivalves (e.g., Dera et al. 2011; Alberti et al. 2012a, 2019). The cause of this difference might include different life habits between the faunal groups, but is still strongly debated in literature (Fürsich et al. 2005; Mutterlose et al. 2010; Alberti et al. 2012a, 2012b; Price et al. 2015; Dera et al. 2016; Hoffmann et al. 2016).

7 Conclusions

The dataset from the Andean Basin in northern Chile is the first stable isotope record of well-dated brachiopod and oyster shells from the Lower Jurassic of South America. The recorded $\delta^{18}O$ values point to warm conditions in the late Sinemurian (average: 27.0 °C), a slight cooling just before the Sinemurian–Pliensbachian transition (average: 24.3 °C), lowest temperatures in the latest Pliensbachian (19.6 °C), and again warmer temperatures in the late Toarcian (average: 24.4 °C). Thereby, the dataset supports the global nature of the Late Pliensbachian Cooling Event. More material is necessary to detect the presumed global warming during the early Toarcian Oceanic Anoxic Event, which was not represented by material in the collection analyzed. The recorded $\delta^{13}C$ values represent background conditions prevalent over most of the Early Jurassic instead of short-term intervals of carbon-cycle perturbations. High-resolution stable isotope ($\delta^{18}O$) analyses of oyster shells point to a seasonality in northern Chile of more than 3 °C in the late Toarcian.

Abbreviations

cl: Clay; g: Gravel; LPCE: Late pliensbachian cooling event; s: Sand; si: Silt; TOAE: Toarcian oceanic anoxic event; VPDB: Vienna pee dee belemnite; VSMOW: Vienna standard mean ocean water

Acknowledgement

The authors thank Winfried Werner for enabling access to the collections of the Bayerische Staatssammlung für Paläontologie und Geologie in Munich, Germany. Birgit Leipner-Mata and Michael Joachimski allowed the use of laboratories at the University of Erlangen-Nürnberg, Germany. Horacio Parent (Rosario, Argentina) and Axel von Hillebrandt (Berlin, Germany) provided copies of scientific articles. The authors thank the Editor-in-Chief Zengzhao Feng

and three anonymous reviewers for their support and constructive comments.

Authors' contributions

MA designed research, performed research, acquired data, and analyzed data. NA performed the stable isotope analyses. MA, FTF, and NA drafted the manuscript. All authors read and approved the final manuscript.

Funding

The study was supported financially by the German Research Foundation (DFG; project AL 1740/3–1).

Availability of data and materials

All data generated and analyzed during this study are included in this published article or in the cited references. The studied material is stored in the collections of the Bayerische Staatssammlung für Paläontologie und Geologie in Munich, Germany.

Competing interests

The authors declare that they have no competing interests.

Author details

[1]Institut für Geowissenschaften, Christian-Albrechts-Universität zu Kiel, Ludewig-Meyn-Straße 10, 24118 Kiel, Germany. [2]GeoZentrum Nordbayern, Fachgruppe PaläoUmwelt, Friedrich-Alexander-Universität Erlangen-Nürnberg, Loewenichstraße 28, 91054 Erlangen, Germany. [3]Leibniz Laboratory for Radiometric Dating and Stable Isotope Research, Christian-Albrechts-Universität zu Kiel, Max-Eyth-Straße 11, 24118 Kiel, Germany.

Received: 12 July 2019 Accepted: 24 October 2019

References

Aberhan, M. 1992. Palökologie und zeitliche Verbreitung benthischer Faunengemeinschaften im Unterjura von Chile. *Beringeria* 5: 3–174.

Aberhan, M. 1993. Faunal replacement in the early Jurassic of northern Chile: Implications for the evolution in Mesozoic benthic shelf ecosystems. *Palaeogeography Palaeoclimatology Palaeoecology* 103: 155–177.

Aberhan, M. 1994. Early Jurassic Bivalvia of northern Chile. Part I. subclasses Palaeotaxodonta, Pteriomorpha, and Isofilibranchia. *Beringeria* 13: 3–115.

Aberhan, M., and T.K. Baumiller. 2003. Selective extinction among early Jurassic bivalves: A consequence of anoxia. *Geology* 31: 1077–1080.

Aberhan, M., and F.T. Fürsich. 1996. Diversity analysis of lower Jurassic bivalves of the Andean basin and the Pliensbachian-Toarcian mass extinction. *Lethaia* 29: 181–195.

Aberhan, M., and A. von Hillebrandt. 1996. Taxonomy, ecology, and palaeobiogeography of *Gervilleioperna* (*Gervilleiognoma*) *aurita* n. subgen. n. Sp. (Bivalvia) from the middle Jurassic of northern Chile. *Paläontologische Zeitschrift* 70: 79–96.

Ait-Itto, F.-Z., G.D. Price, A.A. Addi, D. Chafiki, and I. Mannani. 2017. Bulk-carbonate and belemnite carbon-isotope records across the Pliensbachian-Toarcian boundary on the northern margin of Gondwana (Issouka, middle atlas, Morocco). *Palaeogeography Palaeoclimatology Palaeoecology* 466: 128–136.

Alberti, M., A. Arabas, F.T. Fürsich, N. Andersen, and P. Ziółkowski. 2019. The middle to upper Jurassic stable isotope record of Madagascar: Linking temperature changes with plate tectonics during the break-up of Gondwana. *Gondwana Research* 73: 1–15.

Alberti, M., F.T. Fürsich, A.A. Abdelhady, and N. Andersen. 2017. Middle to late Jurassic equatorial seawater temperatures and latitudinal temperature gradients based on stable isotopes of brachiopods and oysters from Gebel Maghara, Egypt. *Palaeogeography Palaeoclimatology Palaeoecology* 468: 301–313.

Alberti, M., F.T. Fürsich, and D.K. Pandey. 2012a. The Oxfordian stable isotope record ($\delta^{18}O$, $\delta^{13}C$) of belemnites, brachiopods, and oysters from the Kachchh Basin (western India) and its potential for palaeoecologic, palaeoclimatic, and palaeogeographic reconstructions. *Palaeogeography Palaeoclimatology Palaeoecology* 344–345: 49–68.

Alberti, M., F.T. Fürsich, and D.K. Pandey. 2013. Seasonality in low latitudes during the Oxfordian (late Jurassic) reconstructed via high-resolution stable isotope analysis of the oyster *Actinostreon marshi* (J. Sowerby, 1814) from the Kachchh Basin, western India. *International Journal of Earth Sciences* 102: 1321–1336.

Alberti, M., F.T. Fürsich, D.K. Pandey, and M. Ramkumar. 2012b. Stable isotope analyses of belemnites from the Kachchh Basin, western India: Paleoclimatic implications for the middle to late Jurassic transition. *Facies* 58: 261–278.

Al-Suwaidi, A.H., G.N. Angelozzi, F. Baudin, D. Condon, S.E. Damborenea, S.P. Hesselbo, H.C. Jenkyns, M. Manceñido, and A. Riccardi. 2014. Re-evaluating the Toarcian oceanic anoxic event from the southern hemisphere, Neuquén Basin, Argentina. *Beringeria Special Issue* 8: 17–18.

Al-Suwaidi, A.H., G.N. Angelozzi, F. Baudin, S.E. Damborenea, S.P. Hesselbo, H. C. Jenkyns, M.O. Manceñido, and A.C. Riccardi. 2010. First record of the early Toarcian oceanic anoxic event from the southern hemisphere, Neuquén Basin, Argentina. *Journal of the Geological Society London* 167: 633–636.

Al-Suwaidi, A.H., S.P. Hesselbo, S.E. Damborenea, M.O. Manceñido, H.C. Jenkyns, A.C. Riccardi, G.N. Angelozzi, and F. Baudin. 2016. The Toarcian oceanic anoxic event (early Jurassic) in the Neuquén Basin, Argentina: A reassessment of age and carbon isotope stratigraphy. *The Journal of Geology* 124: 171–193.

Anderson, T.F., and M.A. Arthur. 1983. Stable isotopes of oxygen and carbon and their application to sedimentological and paleoenvironmental problems. In *Stable isotopes in sedimentary geology. SEPM Short Course*, ed. M.A. Arthur, T.F. Anderson, I.R. Kaplan, J. Veizer, and L. Land, vol. 10, 1–151.

Arabas, A. 2016. Middle-upper Jurassic stable isotope records and seawater temperature variations: New palaeoclimate data from marine carbonate and belemnite rostra (Pieniny Klippen Belt, Carpathians). *Palaeogeography Palaeoclimatology Palaeoecology* 446: 284–294.

Arabas, A., J. Schlögl, and C. Meister. 2017. Early Jurassic carbon and oxygen isotope records and seawater temperature variations: Insights from marine carbonate and belemnite rostra (Pieniny Klippen Belt, Carpathians). *Palaeogeography Palaeoclimatology Palaeoecology* 485: 119–135.

Armendáriz, M., I. Rosales, B. Bádenas, M. Aurell, J.C. García-Ramos, and L. Piñuela. 2012. High-resolution chemostratigraphic records from lower Pliensbachian belemnites: Palaeoclimatic perturbations, organic facies and water mass exchange (Asturian basin, northern Spain). *Palaeogeography Palaeoclimatology Palaeoecology* 333–334: 178–191.

Baeza-Carratalá, J.F. 2013. Diversity patterns of early Jurassic brachiopod assemblages from the westernmost Tethys (eastern Subbetic). *Palaeogeography Palaeoclimatology Palaeoecology* 381–382: 76–91.

Bailey, T.R., Y. Rosenthal, J.M. McArthur, B. van de Schootbrugge, and M.F. Thirlwall. 2003. Paleoceanographic changes of the late Pliensbachian-early Toarcian interval: A possible link to the genesis of an oceanic anoxic event. *Earth and Planetary Science Letters* 212: 307–320.

Barbin, V. 2013. Application of cathodoluminescence microscopy to recent and past biological materials: A decade of progress. *Mineralogy and Petrology* 107: 353–362.

Bodin, S., F.-N. Krencker, T. Kothe, R. Hoffmann, E. Mattioli, U. Heimhofer, and L. Kabiri. 2016. Perturbation of the carbon cycle during the late Pliensbachian – Early Toarcian: New insight from high-resolution carbon isotope records in Morocco. *Journal of African Earth Sciences* 116: 89–104.

Bougeault, C., P. Pellenard, J.-F. Deconinck, S.P. Hesselbo, J.-L. Dommergues, L. Bruneau, T. Cocquerez, R. Laffont, E. Huret, and N. Thibault. 2017. Climatic and palaeoceanographic changes during the Pliensbachian (early Jurassic) inferred from clay mineralogy and stable isotope (C-O) geochemistry (NW Europe). *Global and Planetary Change* 149: 139–152.

Boulila, S., and L.A. Hinnov. 2017. A review of tempo and scale of the early Jurassic Toarcian OAE: Implications for carbon cycle and sea level variations. *Newsletters on Stratigraphy* 50: 363–389.

Bowen, R. 1963. O^{18}/O^{16} paleotemperature measurements on Mesozoic Belemnoidea from Neuquen and Santa Cruz provinces, Argentina. *Journal of Paleontology* 37: 714–718.

Caruthers, A.H., D.R. Gröcke, and P.L. Smith. 2011. The significance of an early Jurassic (Toarcian) carbon-isotope excursion in Haida Gwaii (Queen Charlotte Islands), British Columbia, Canada. *Earth and Planetary Science Letters* 307: 19–26.

Caswell, B.A., and A.L. Coe. 2012. A high-resolution shallow marine record of the Toarcian (early Jurassic) oceanic anoxic event from the east midlands shelf, UK. *Palaeogeography, Palaeoclimatology, Palaeoecology* 365–366: 124–135.

Cecca, F., and F. Macchioni. 2004. The two early Toarcian (early Jurassic) extinction events in ammonoids. *Lethaia* 37: 35–56.

Chandler, M.A., D. Rind, and R. Ruedy. 1992. Pangaean climate during the early Jurassic: GCM simulations and the sedimentary record of paleoclimate. *Geological Society of America Bulletin* 104: 543–559.

Cresta, S., A. Goy, S. Ureta, C. Arias, E. Barrón, J. Bernad, M.L. Canales, F. García-Joral, E. García-Romero, P.R. Gialanella, J.J. Gómez, J.A. González, C. Herrero, G. Martínez, M.L. Osete, N. Perilli, and J.J. Villalaín. 2001. The global boundary Stratotype section and point (GSSP) of the Toarcian-Aalenian boundary (lower-middle Jurassic). *Episodes* 24: 166–175.

Danise, S., R.J. Twitchett, C.T.S. Little, and M.-E. Clémence. 2013. The impact of global warming and anoxia on marine benthic community dynamics: An example from the Toarcian (early Jurassic). *PLoS One* 8: e56255.

Dera, G., B. Brigaud, F. Monna, R. Laffont, E. Pucéat, J.-F. Deconinck, P. Pellenard, M.M. Joachimski, and C. Durlet. 2011. Climatic ups and downs in a disturbed Jurassic world. *Geology* 39: 215–218.

Dera, G., and Y. Donnadieu. 2012. Modeling evidences for global warming, Arctic seawater freshening, and sluggish oceanic circulation during the early Toarcian anoxic event. *Paleoceanography* 27: PA2211.

Dera, G., P. Neige, J.-L. Dommergues, E. Fara, R. Laffont, and P. Pellenard. 2010. High-resolution dynamics of early Jurassic marine extinctions: The case of Pliensbachian-Toarcian ammonites (Cephalopoda). *Journal of the Geological Society London* 167: 21–33.

Dera, G., P. Pellenard, P. Neige, J.-F. Deconinck, E. Pucéat, and J.-L. Dommergues. 2009a. Distribution of clay minerals in early Jurassic Peritethyan seas: Palaeoclimatic significance inferred from multiproxy comparisons. *Palaeogeography Palaeoclimatology Palaeoecology* 271: 39–51.

Dera, G., E. Pucéat, P. Pellenard, P. Neige, D. Delsate, M.M. Joachimski, L. Reisberg, and M. Martinez. 2009b. Water mass exchange and variations in seawater temperature in the NW Tethys during the early Jurassic: Evidence from neodymium and oxygen isotopes of fish teeth and belemnites. *Earth and Planetary Science Letters* 286: 198–207.

Dera, G., A. Toumoulin, and K. de Baets. 2016. Diversity and morphological evolution of Jurassic belemnites from South Germany. *Palaeogeography, Palaeoclimatology, Palaeoecology* 457: 80–97.

Dromart, G., J.-P. Garcia, S. Picard, F. Atrops, C. Lécuyer, and S.M.F. Sheppard. 2003. Ice age at the middle-late Jurassic transition? *Earth and Planetary Science Letters* 213: 205–220.

Epstein, S., R. Buchsbaum, H.A. Lowenstam, and H.C. Urey. 1951. Carbonate-water isotopic temperature scale. *Geological Society of America Bulletin* 62: 417–426.

Fantasia, A., K.B. Föllmi, T. Adatte, E. Bernárdez, J.E. Spangenberg, and E. Mattioli. 2018. The Toarcian oceanic anoxic event in southwestern Gondwana: An example from the Andean basin, northern Chile. *Journal of the Geological Society London* 175: 883–902.

Fürsich, F.T., I.B. Singh, M. Joachimski, S. Krumm, M. Schlirf, and S. Schlirf. 2005. Palaeoclimatic reconstructions of the middle Jurassic of Kachchh (western India): An integrated approach based on palaeoecological, oxygen isotopic, and clay mineralogical data. *Palaeogeography Palaeoclimatology Palaeoecology* 217: 289–309.

Gómez, J.J., and C. Arias. 2010. Rapid warming and ostracods mass extinction at the lower Toarcian (Jurassic) of Central Spain. *Marine Micropaleontology* 74: 119–135.

Gómez, J.J., M.J. Comas-Rengifo, and A. Goy. 2016. Palaeoclimatic oscillations in the Pliensbachian (early Jurassic) of the Asturian Basin (northern Spain). *Climate of the Past* 12: 1199–1214.

Gómez, J.J., A. Goy, and M.L. Canales. 2008. Seawater temperature and carbon isotope variations in belemnites linked to mass extinction during the Toarcian (early Jurassic) in central and northern Spain. Comparison with other European sections. *Palaeogeography, Palaeoclimatology, Palaeoecology* 258: 28–58.

Gröcke, D.R., R.S. Hori, J. Trabucho-Alexandre, D.B. Kemp, and L. Schwark. 2011. An open ocean record of the Toarcian oceanic anoxic event. *Solid Earth* 2: 245–257.

Gröschke, M., A. von Hillebrandt, P. Prinz, L.A. Quinzio, and H.-G. Wilke. 1988. Marine Mesozoic paleogeography in northern Chile between 21°-26°S. In *The Southern Central Andes. Lecture Notes in Earth Sciences*, ed. H. Bahlburg, C. Breitkreuz, and P. Giese, vol. 17, 105–117.

Hallam, A. 2001. A review of the broad pattern of Jurassic Sea-level changes and their possible causes in the light of current knowledge. *Palaeogeography Palaeoclimatology Palaeoecology* 167: 23–37.

Harazim, D., B. van de Schootbrugge, K. Sorichter, J. Fiebig, A. Weug, G. Suan, and W. Oschmann. 2013. Spatial variability of watermass conditions within the European Epicontinental seaway during the early Jurassic (Pliensbachian-Toarcian). *Sedimentology* 60: 359–390.

Hesselbo, S.P., D.R. Gröcke, H.C. Jenkyns, C.J. Bjerrum, P. Farrimond, H.S. Morgans Bell, and O.R. Green. 2000a. Massive dissociation of gas hydrate during a Jurassic oceanic anoxic event. *Nature* 406: 392–395.

Hesselbo, S.P., H.C. Jenkyns, L.V. Duarte, and L.C.V. Oliveira. 2007. Carbon-isotope record of the early Jurassic (Toarcian) oceanic anoxic event from fossil wood and marine carbonate (Lusitanian Basin, Portugal). *Earth and Planetary Science Letters* 253: 455–470.

Hesselbo, S.P., C. Meister, and D.R. Gröcke. 2000b. A potential global stratotype for the Sinemurian-Pliensbachian boundary (lower Jurassic), Robin Hood's bay, UK: Ammonite faunas and isotope stratigraphy. *Geological Magazine* 137: 601–607.

Hodgson, W.A. 1966. Carbon and oxygen isotope ratios in diagenetic carbonates from marine sediments. *Geochimica et Cosmochimica Acta* 30: 1223–1233.

Hoffmann, R., D.K. Richter, R.D. Neuser, N. Jöns, B.J. Linzmeier, R.E. Lemanis, F. Fusseis, X. Xiao, and A. Immenhauser. 2016. Evidence for a composite organic-inorganic fabric of belemnite rostra: Implications for palaeoceanography and palaeoecology. *Sedimentary Geology* 341: 203–215.

Huang, C., and S.P. Hesselbo. 2014. Pacing of the Toarcian oceanic anoxic event (early Jurassic) from astronomical correlation of marine sections. *Gondwana Research* 25: 1348–1356.

Hudson, J.D. 1977. Stable isotopes and limestone lithification. *Journal of the Geological Society, London* 133: 637–660.

Jenkyns, H.C. 1988. The early Toarcian (Jurassic) anoxic event: Stratigraphic, sedimentary, and geochemical evidence. *American Journal of Science* 288: 101–151.

Jenkyns, H.C., C.E. Jones, D.R. Gröcke, S.P. Hesselbo, and D.N. Parkinson. 2002. Chemostratigraphy of the Jurassic system: Applications, limitations and implications for palaeoceanography. *Journal of the Geological Society, London* 159: 351–378.

Kemp, D.B., and K. Izumi. 2014. Multiproxy geochemical analysis of a Panthalassic margin record of the early Toarcian oceanic anoxic event (Toyora area, Japan). *Palaeogeography, Palaeoclimatology, Palaeoecology* 414: 332–341.

Korte, C., and S.P. Hesselbo. 2011. Shallow marine carbon and oxygen isotope and elemental records indicate icehouse-greenhouse cycles during the early Jurassic. *Paleoceanography* 26: PA4219.

Korte, C., S.P. Hesselbo, H.C. Jenkyns, R.E.M. Rickaby, and C. Spötl. 2009. Palaeoenvironmental significance of carbon- and oxygen-isotope stratigraphy of marine Triassic-Jurassic boundary sections in SW Britain. *Journal of the Geological Society, London* 166: 431–445.

Korte, C., S.P. Hesselbo, C.V. Ullmann, G. Dietl, M. Ruhl, G. Schweigert, and N. Thibault. 2015. Jurassic climate mode governed by ocean gateway. *Nature Communications* 6: 10015.

Krencker, F.N., S. Bodin, R. Hoffmann, G. Suan, E. Mattioli, L. Kabiri, K.B. Föllmi, and A. Immenhauser. 2014. The middle Toarcian cold snap: Trigger of mass extinction and carbonate factory demise. *Global and Planetary Change* 117: 64–78.

Krencker, F.-N., S. Bodin, G. Suan, U. Heimhofer, L. Kabiri, and A. Immenhauser. 2015. Toarcian extreme warmth led to tropical cyclone intensification. *Earth and Planetary Science Letters* 425: 120–130.

Li, Q., J.M. McArthur, and T.C. Atkinson. 2012. Lower Jurassic belemnites as indicators of palaeo-temperature. *Palaeogeography, Palaeoclimatology, Palaeoecology* 315–316: 38–45.

Littler, K., S.P. Hesselbo, and H.C. Jenkyns. 2010. A carbon-isotope perturbation at the Pliensbachian-Toarcian boundary: Evidence from the Lias group, NE England. *Geological Magazine* 147: 181–192.

Manceñido, M.O. 1981. A revision of early Jurassic Spiriferinidae (Brachiopoda, Spiriferida) from Argentina. In *Cuencas sedimentarias del Jurásico y Cretácico de América del Sur*, ed. W. Volkheimer and E. Musacchio, vol. 2, 625–660.

Manceñido, M.O., and A.S. Dagys. 1992. Brachiopods of the circum-Pacific region. In *The Jurassic of the Circum-Pacific*, ed. G.E.G. Westermann, 328–333.

Martinez, M., and G. Dera. 2015. Orbital pacing of carbon fluxes by a ~9-my eccentricity cycle during the Mesozoic. *Proceedings of the National Academy of Sciences* 112: 12604–12609.

Mazzini, A., H. Svensen, H.A. Leanza, F. Corfu, and S. Planke. 2010. Early Jurassic shale chemostratigraphy and U-Pb ages from the Neuquén Basin (Argentina): Implications for the Toarcian oceanic anoxic event. *Earth and Planetary Science Letters* 297: 633–645.

McArthur, J.M., D.T. Donovan, M.F. Thirlwall, B.W. Fouke, and D. Mattey. 2000. Strontium isotope profile of the early Toarcian (Jurassic) oceanic anoxic event, the duration of ammonite biozones, and belemnite palaeotemperatures. *Earth and Planetary Science Letters* 179: 269–285.

McArthur, J.M., P. Doyle, M.J. Leng, K. Reeves, C.T. Williams, R. Garcia-Sanchez, and R.J. Howarth. 2007. Testing palaeo-environmental proxies in Jurassic belemnites: Mg/Ca, Sr/Ca, Na/Ca, $\delta^{18}O$ and $\delta^{13}C$. *Palaeogeography Palaeoclimatology Palaeoecology* 252: 464–480.

Menini, A., E. Mattioli, J.E. Spangenberg, B. Pittet, and G. Suan. 2019. New calcareous nannofossil and carbon isotope data for the Pliensbachian/Toarcian boundary (early Jurassic) in the western Tethys and their paleoenvironmental implications. *Newsletters on Stratigraphy* 52: 173–196.

Mercuzot, M., P. Pellenard, C. Durlet, C. Bougeault, C. Meister, J.-L. Dommergues, N. Thibault, F. Baudin, O. Mathieu, L. Bruneau, E. Huret, and K. El Hmidi. 2019. Carbon-isotope events during the Pliensbachian (lower Jurassic) on the African and European margins of the NW Tethyan realm. *Newsletters on Stratigraphy*, in press.

Metodiev, L., and E. Koleva-Rekalova. 2008. Stable isotope records ($\delta^{18}O$ and $\delta^{13}C$) of lower-middle Jurassic belemnites from the Western Balkan mountains (Bulgaria): Palaeoenvironmental application. *Applied Geochemistry* 23: 2845–2856.

Metodiev, L.S., I.P. Savov, D.R. Gröcke, P.B. Wignall, R.J. Newton, P.V. Andreeva, and E.K. Koleva-Rekalova. 2014. Paleoenvironmental conditions recorded by $^{87}Sr/^{86}Sr$, $\delta^{13}C$, and $\delta^{18}O$ in late Pliensbachian-Toarcian (Jurassic) belemnites from Bulgaria. *Palaeogeography Palaeoclimatology Palaeoecology* 409: 98–113.

Mettraux, M., H. Weissert, and P. Homewood. 1989. An oxygen-minimum palaeoceanographic signal from early Toarcian cavity fills. *Journal of the Geological Society, London* 146: 333–344.

Mutterlose, J., M. Malkoc, S. Schouten, J.S. Sinninghe Damsté, and A. Forster. 2010. TEX_{86} and stable $\delta^{18}O$ paleothermometry of early cretaceous sediments: Implications for belemnite ecology and paleotemperature proxy application. *Earth and Planetary Science Letters* 298: 286–298.

Nelson, C.S., and A.M. Smith. 1996. Stable oxygen and carbon isotope compositional fields for skeletal and diagenetic components in New Zealand Cenozoic nontropical carbonate sediments and limestones: A synthesis and review. *New Zealand Journal of Geology and Geophysics* 39: 93–107.

Nori, L., and B. Lathuilière. 2003. Form and environment of *Gryphaea arcuata*. *Lethaia* 36: 83–96.

Pálfy, J., and P.L. Smith. 2000. Synchrony between early Jurassic extinction, oceanic anoxic event, and the Karoo-Ferrar flood basalt volcanism. *Geology* 28: 747–750.

Pérez, E. 1982. Bioestratigrafía del Jurásico de Quebrada Asientos, Norte de Potrerillos, Región de Atacama. *Servicio Nacional de Geología y Minería Boletin* 37: 1–149.

Pérez, E., M. Aberhan, R. Reyes, and A. von Hillebrandt. 2008. Early Jurassic Bivalvia of northern Chile. Part III. Order Trigonioida. *Beringeria* 39: 51–102.

Price, G.D. 1999. The evidence and implications of polar ice during the Mesozoic. *Earth-Science Reviews* 48: 183–210.

Price, G.D. 2010. Carbon-isotope stratigraphy and temperature change during the early-middle Jurassic (Toarcian-Aalenian), Raasay, Scotland, UK. *Palaeogeography Palaeoclimatology Palaeoecology* 285: 255–263.

Price, G.D., S.J. Baker, J. VanDeVelde, and M.-E. Clémence. 2016. High-resolution carbon cycle and seawater temperature evolution during the early Jurassic (Sinemurian-early Pliensbachian). *Geochemistry Geophysics Geosystems* 17: 3917–3928.

Price, G.D., M.B. Hart, P.R. Wilby, and K.N. Page. 2015. Isotopic analysis of Jurassic (Callovian) mollusks from the Christian Malford Lagerstätte (UK): Implications for ocean water temperature estimates based on belemnoids. *Palaios* 30: 645–654.

Rees, P.M., A.M. Ziegler, and P.J. Valdes. 2000. Jurassic phytogeography and climates: New data and model comparisons. In *Warm climates in earth history*, ed. B.T. Huber, K.G. Macleod, and S.L. Wing, 297–318.

Riccardi, A.C. 2008. The marine Jurassic of Argentina: A biostratigraphic framework. *Episodes* 31: 326–335.

Riding, J.B., M.J. Leng, S. Kender, S.P. Hesselbo, and S. Feist-Burkhardt. 2013. Isotopic and palynological evidence for a new early Jurassic environmental perturbation. *Palaeogeography, Palaeoclimatology, Palaeoecology* 374: 16–27.

Rodríguez-Tovar, F.J., and M. Reolid. 2013. Environmental conditions during the Toarcian oceanic anoxic event (T-OAE) in the westernmost Tethys: Influence of the regional context on a global phenomenon. *Bulletin of Geosciences* 88: 697–712.

Rosales, I., A. Barnolas, A. Goy, A. Sevillano, M. Armendáriz, and J.M. López-García. 2018. Isotope records (C-O-Sr) of late Pliensbachian-early Toarcian environmental perturbations in the westernmost Tethys (Majorca Island, Spain). *Palaeogeography, Palaeoclimatology, Palaeoecology* 497: 168–185.

Rosales, I., S. Quesada, and S. Robles. 2004a. Paleotemperature variations of early Jurassic seawater recorded in geochemical trends of belemnites from the Basque-Cantabrian basin, northern Spain. *Palaeogeography, Palaeoclimatology, Palaeoecology* 203: 253–275.

Rosales, I., S. Robles, and S. Quesada. 2004b. Elemental and oxygen isotope composition of early Jurassic belemnites: Salinity vs. temperature signals. *Journal of Sedimentary Research* 74: 342–354.

Ros-Franch, S., J. Echevarría, S.E. Damborenea, M.O. Manceñido, H.C. Jenkyns, A. Al-Suwaidi, S.P. Hesselbo, and A.C. Riccardi. 2019. Population response during an oceanic anoxic event: The case of Posidonotis (Bivalvia) from the lower Jurassic of Neuquén Basin, Argentina. *Palaeogeography Palaeoclimatology Palaeoecology* 525: 57–67.

Ruhl, M., S.P. Hesselbo, L. Hinnov, H.C. Jenkyns, W. Xu, J.B. Riding, M. Storm, D. Minisini, C.V. Ullmann, and M.J. Leng. 2016. Astronomical constraints on the duration of the early Jurassic Pliensbachian stage and global climatic fluctuations. *Earth and Planetary Science Letters* 455: 149–165.

Sælen, G., P. Doyle, and M.R. Talbot. 1996. Stable-isotope analyses of belemnite rostra from the Whitby mudstone Fm., England: Surface water conditions during deposition of a marine black shale. *Palaios* 11: 97–117.

Schmid-Röhl, A., H.-J. Röhl, W. Oschmann, A. Frimmel, and L. Schwark. 2002. Palaeoenvironmental reconstruction of lower Toarcian epicontinental black shales (Posidonia shale, SW Germany): Global versus regional control. *Geobios* 35: 13–20.

Sellwood, B.W., and P.J. Valdes. 2006. Mesozoic climates: General circulation models and the rock record. *Sedimentary Geology* 190: 269–287.

Shackleton, N.J., and J.P. Kennett. 1975. Paleotemperature history of the Cenozoic and the initiation of Antarctic glaciation: Oxygen and carbon isotope analyses in DSDP sites 277, 279, and 281. *Initial Reports of the Deep Sea Drilling Project* 29: 743–755.

Silva, R.L., and L.V. Duarte. 2015. Organic matter production and preservation in the Lusitanian Basin (Portugal) and Pliensbachian climatic hot snaps. *Global and Planetary Change* 131: 24–34.

Silva, R.L., L.V. Duarte, M.J. Comas-Rengifo, J.G. Mendonça Filho, and A.C. Azerêdo. 2011. Update of the carbon and oxygen isotopic records of the early-late Pliensbachian (early Jurassic, ~187Ma): Insights from the

organic-rich hemipelagic series of the Lusitanian Basin (Portugal). *Chemical Geology* 283: 177–184.

Suan, G., E. Mattioli, B. Pittet, C. Lécuyer, B. Suchéras-Marx, L.V. Duarte, M. Philippe, L. Reggiani, and F. Martineau. 2010. Secular environmental precursors to early Toarcian (Jurassic) extreme climate changes. *Earth and Planetary Science Letters* 290: 448–458.

Suan, G., E. Mattioli, B. Pittet, S. Mailliot, and C. Lécuyer. 2008. Evidence for major environmental perturbation prior to and during the Toarcian (early Jurassic) oceanic anoxic event from the Lusitanian Basin, Portugal. *Paleoceanography* 23: PA1202.

Suan, G., B.L. Nikitenko, M.A. Rogov, F. Baudin, J.E. Spangenberg, V.G. Knyazev, L.A. Glinskikh, A.A. Goryacheva, T. Adatte, J.B. Riding, K.B. Föllmi, B. Pittet, E. Mattioli, and C. Lécuyer. 2011. Polar record of early Jurassic massive carbon injection. *Earth and Planetary Science Letters* 312: 102–113.

Teichert, B.M.A., and F.W. Luppold. 2013. Glendonites from an early Jurassic methane seep — Climate or methane indicators? *Palaeogeography, Palaeoclimatology, Palaeoecology* 390: 81–93.

Ullmann, C.V., and C. Korte. 2015. Diagenetic alteration in low-mg calcite from macrofossils: A review. *Geological Quarterly* 59: 3–20.

Ullmann, C.V., N. Thibault, M. Ruhl, S.P. Hesselbo, and C. Korte. 2014. Effect of a Jurassic oceanic anoxic event on belemnite ecology and evolution. *Proceedings of the National Academy of Sciences* 111: 10073–10076.

Urey, H.C., H.A. Lowenstam, S. Epstein, and C.R. McKinney. 1951. Measurement of paleotemperatures and temperatures of the upper cretaceous of England, Denmark, and the southeastern United States. *Geological Society of America Bulletin* 62: 399–416.

Valdes, P.J., and B.W. Sellwood. 1992. A palaeoclimate model for the Kimmeridgian. *Palaeogeography, Palaeoclimatology, Palaeoecology* 95: 47–72.

van de Schootbrugge, B., T.R. Bailey, Y. Rosenthal, M.E. Katz, J.D. Wright, K.G. Miller, S. Feist-Burkhardt, and P.G. Falkowski. 2005b. Early Jurassic climate change and the radiation of organic-walled phytoplankton in the Tethys Ocean. *Paleobiology* 31: 73–97.

van de Schootbrugge, B., J.M. McArthur, T.R. Bailey, Y. Rosenthal, J.D. Wright, and K.G. Miller. 2005a. Toarcian oceanic anoxic event: An assessment of global causes using belemnite C isotope records. *Paleoceanography* 20: PA3008.

van Hinsbergen, D.J.J., L.V. de Groot, S.J. van Schalk, W. Spakman, P.K. Bijl, A. Sluijs, C.G. Langereis, and H. Brinkhuis. 2015. A paleolatitude calculator for paleoclimate studies. *PLoS One* 10: e0126946.

Vicente, J.-C. 2006. Dynamic paleogeography of the Jurassic Andean basin: Pattern of regression and general considerations on main features. *Revista de la Asociación Geológica Argentina* 61: 408–437.

Volkheimer, W., O.W.M. Rauhut, M.E. Quattrocchio, and M.A. Martinez. 2008. Jurassic paleoclimates in Argentina, a review. *Revista de la Asociación Geológica Argentina* 63: 549–556.

von Hillebrandt, A. 1971. Der Jura in der chilenisch-argentinischen Hochkordillere (25° bis 32°30′ S). *Münstersche Forschungen zur Geologie und Paläontologie* 20 (21): 63–87.

von Hillebrandt, A. 1973. Neue Ergebnisse über den Jura in Chile und Argentinien. *Münstersche Forschungen zur Geologie und Paläontologie* 31 (32): 167–199.

von Hillebrandt, A. 1987. Liassic ammonite zones of South America and correlations with other provinces. With description of new genera and species of ammonites. In *Bioestratigrafia de los Sistemas Regionales del Jurásico y Cretácico de América del Sur*, ed. W. Volkheimer, vol. 1, 111–157.

von Hillebrandt, A. 2002. Ammoniten aus dem oberen Sinemurium von Südamerika. *Revue de Paléobiologie* 21: 35–147.

von Hillebrandt, A. 2006. Ammoniten aus dem Pliensbachium (Carixium und Domerium) von Südamerika. *Revue de Paléobiologie* 25: 1–403.

von Hillebrandt, A., and R. Schmidt-Effing. 1981. Ammoniten aus dem Toarcium (Jura) von Chile (Südamerika). *Zitteliana* 6: 3–74.

Wierzbowski, H. 2002. Detailed oxygen and carbon isotope stratigraphy of the Oxfordian in Central Poland. *International Journal of Earth Sciences* 91: 304–314.

Wierzbowski, H. 2004. Carbon and oxygen isotope composition of Oxfordian-early Kimmeridgian belemnite rostra: Palaeoenvironmental implications for late Jurassic seas. *Palaeogeography, Palaeoclimatology, Palaeoecology* 203: 153–168.

Wierzbowski, H., K. Dembicz, and T. Praszkier. 2009. Oxygen and carbon isotope composition of Callovian-lower Oxfordian (middle-upper Jurassic) belemnite rostra from Central Poland: A record of a late Callovian global sea-level rise? *Palaeogeography, Palaeoclimatology, Palaeoecology* 283: 182–194.

Wierzbowski, H., and M. Joachimski. 2007. Reconstruction of late Bajocian-Bathonian marine palaeoenvironments using carbon and oxygen isotope ratios of calcareous fossils from the polish Jura chain (Central Poland). *Palaeogeography, Palaeoclimatology, Palaeoecology* 254: 523–540.

Yi, H., L. Chen, H.C. Jenkyns, X. Da, M. Xia, G. Xu, and C. Ji. 2013. The early Jurassic oil shales in the Qiangtang Basin, northern Tibet: Biomarkers and Toarcian oceanic anoxic events. *Oil Shale* 30: 441–455.

Publisher's Note